Hindawi
International Journal of Intelligent Systems
Volume 2023, Article ID 9926188, 24 pages
https://doi.org/10.1155/2023/9926188

*Research Article*

# Adaptive-Neuro-Learning Tracking Control for the Permanent Magnet Synchronous Motor with Full-State Prescribed Performances and Time Delays

**Tandong Li**,[1] **Shaobo Li**,[1,2] **Junxing Zhang**,[2] **Hang Sun**,[3] **Chaojie Zheng**,[1] **and Dongchao Lv**[1]

[1]*School of Mechanical Engineering, Guizhou University, Guiyang, China*
[2]*State Key Laboratory of Public Big Data, Guizhou University, Guiyang, China*
[3]*Guizhou Agricultural Sciences, Guizhou Provincial Academy of Agricultural Sciences, Guiyang, China*

Correspondence should be addressed to Shaobo Li; lishaobo@gzu.edu.cn

Received 26 February 2023; Revised 5 June 2023; Accepted 12 June 2023; Published 21 September 2023

Academic Editor: Vasudevan Rajamohan

Copyright © 2023 Tandong Li et al. This is an open access article distributed under the Creative Commons Attribution License, which permits unrestricted use, distribution, and reproduction in any medium, provided the original work is properly cited.

High-performance tracking control is essential for permanent magnet synchronous motors in the perturbed environment. Given this, a new hybrid controller is proposed in this study for a permanent magnet synchronous motor with load disturbances as well as time delays. First, a new prescribed performance method is proposed to achieve the full-state performance constraints with load disturbances. Second, a time-varying filter is proposed for the first time to avoid the "complexity explosion" problem of the backstepping method while guaranteeing the convergence of the filtering error. Third, by combining Lyapunov–Krasovskii functionals with adaptive neural networks, the time-delay disturbance and unknown nonlinear dynamics of the control system have been solved. The stability analysis proves that all signals in the closed-loop system are bounded. To show the effectiveness of the intelligent controller, the comparison simulations are given to confirm the advantages of the proposed adaptive neural control scheme.

## 1. Introduction

Owing to the advantages of small volume, high efficiency, and reliability, permanent magnet synchronous motors (PMSMs) are broadly adopted in various industrial applications [1–4]. However, PMSMs are nonlinear coupling systems making the controller design more challenging [5, 6]. Recently, increasing control methods have been constructed for PMSMs, such as sliding mode control [7–10], adaptive fuzzy control [11–13], adaptive neural network control [14, 15], and backstepping control [4, 16, 17]. Even so, the preceding methods rarely focus on the tracking issue of the PMSMs with uncertain nonlinearities, full-state constraints, and time delays.

The system with uncertain dynamics is very difficult to control by traditional methods [18, 19]. Recently, neural networks (NNs) are popularly adopted to learn uncertainties in the control system [20]. Furthermore, the backstepping methods are systematic and powerful tools to integrate fuzzy logical systems or neural networks [21–24]. For these reasons, this study employs the backstepping framework incorporating neural networks to design the controller. Nevertheless, backstepping-based strategies are susceptible to the "explosion of complexity" produced by the iterative derivations of virtual control laws [11]. To solve this issue, the dynamic surface control (DSC) is constructed by employing the first-order filters in the works of Yu et al. [25] and Gao et al. [21]. To eliminate the effect of the filtering error on the system, compensation signals are introduced in the work of Yu et al. [26]. The conventional DSC methods require eliminating the effect of the filtering error, which makes the controller more or less complex. Thus, a neuro-learning-based dynamic surface control is considered in this study using a time-varying filter and radial basis neural

networks (RBFNNs) to solve the "complexity explosion" problem and ever-presenting uncertainties.

Additionally, full-state constraints are often taken into account for practical PMSMs to ensure safe operation and control performance. Regarding state constraints, significant achievements have been implemented, such as barrier Lyapunov functions (BLFs) [27, 28] and prescribed performance control (PPC) [29–32]. Among these methods, PPC is regarded as a promising method to enhance the tracking performance of the system. For example, in the works of Dai et al. [9], Jia et al. [33], and Hua et al. [32], the traditional exponential performance function has been adopted to ensure the prescribed performance of the systems. The work of Wang and Hu [34] considers the high-frequency changing of the reference signal by presenting a hyperbolic-cosecant-type performance function. Backstepping control decomposes complex nonlinear systems into multiple simpler and lower-order systems by introducing virtual control. The states in the subsystem need to track the virtual control law, which means that the prescribed performances of the subsystems are important. Furthermore, external load perturbations may degrade the tracking ability of the PMSM system so that tracking errors may exceed the constraint bounds. However, the full-state prescribed performance and the effect of load oscillations have rarely been considered in previous works. Therefore, it is another motivation for this study to study the full-state prescribed performance tracking control with external load effects.

Apart from the challenges mentioned previously, another noteworthy concern is the impact of time delays in the regular controller design, which may cause instability or damage to the system [35]. To compensate for the time delays of control systems, the common tools are Lyapunov–Krasovskii functionals (LKFs). For instance, in the study of Wang et al. [31], LKFs are established to eliminate the delayed states for nonlinear systems. The unknown time-delay terms of pure-feedback switched systems are compensated by LKFs in the work of Niu et al. [36]. Although the preceding studies can effectively deal with time delays and enhance control performance, they are not currently considered in the prescribed performance control of the PMSMs. Therefore, this study prefers to deal with time delays for the PMSM by constructing appropriate LKFs.

Motivated by the former discussions, a neuro-learning-based adaptive prescribed performance control (NPPC) is proposed for the PMSM with full-state constraints and time delays by the DSC method. Compared with the existing results on controlling the PMSM, the major contributions in this study are concluded as follows:

(1) Compared with references [9, 32], this study proposes a novel performance control scheme, which can ensure the full-state performances of the system with external load disturbances

(2) Unlike the conventional backstepping methods [21, 26] employing the first-order filter, this study proposes a time-varying filter for the first time, to solve the issue of "complexity explosion" while guaranteeing convergence of the filtering error and faster filtering speed

(3) An adaptive-neuro-learning tracking controller for the PMSM with time delays is proposed, in which the unknown nonlinear dynamics of the system are approximated by constructing the RBFNNs, and the weights of RBFNNs are adjusted online by the designed adaptive laws

The remainder of this article is organized as follows. Section 2 delivers the statements of problem formulation and preliminaries. Section 3 provides the detailed controller design process. Section 4 presents the stability analysis. Simulation results are provided in Section 5. Finally, the conclusions are presented in Section 6.

## 2. Problem Formulation and Preliminaries

The dynamic mathematical model of the PMSM [14] in $d-q$ rotating coordinates can be expressed as

$$\begin{cases} \dfrac{\mathrm{d}\theta}{\mathrm{d}t} = \omega, \\ J\dfrac{\mathrm{d}\omega}{\mathrm{d}t} = \dfrac{3}{2}n_p\left(\left(L_d - L_q\right)i_d i_q + \varphi_f i_q\right) - B\omega - x_{\mathrm{TL}}, \\ L_q\dfrac{\mathrm{d}i_q}{\mathrm{d}t} = -R_s i_q - L_d n_p \omega \varphi_f + u_q, \\ L_d\dfrac{\mathrm{d}i_d}{\mathrm{d}t} = -R_s i_d - L_q n_p \omega i_q + u_d, \end{cases} \tag{1}$$

where the parameters are listed in Table 1.

For simplifying the dynamic mathematical model of the PMSM, we define variables $x_1 = \theta, x_2 = \omega, x_3 = i_q, x_4 = i_d$. Then, taking time delays into account, (1) can be rewritten as

$$\begin{cases} \dot{x}_1 = x_2 + \chi_1\left(\overline{x}_1\left(t-\sigma_1\right)\right), \\ \dot{x}_2 = a_1 x_2 + a_2 x_3 + a_3 x_3 x_4 - \dfrac{x_{TL}}{J} + \chi_2\left(\overline{x}_2\left(t-\sigma_2\right)\right), \\ \cdot\ \dot{x}_3 = b_1 x_3 + b_2 x_2 x_4 + b_3 x_2 + b_4 u_q + \chi_3\left(\overline{x}_3\left(t-\sigma_3\right)\right), \\ \cdot\ \dot{x}_4 = c_1 x_4 + c_2 x_2 x_3 + c_3 u_d + \chi_4\left(\overline{x}_4\left(t-\sigma_4\right)\right), \end{cases} \tag{2}$$

where $\overline{x}_i(t) = (x_1(t), \cdots, x_i(t))^T \in R^i, i = 1, \cdots, 4$, $\chi_i(\overline{x}_i(t-\sigma_i))$ represent the time-delay terms, $\sigma_i$ are positive constants, and $a_1 = -B/J, a_2 = 1.5n_p\varphi_f/J, a_3 = 1.5n_P\ (L_d - L_q)/J, b_1 = -R_s/L_q,\quad b_2 = -L_d n_p/L_q, b_3 = -n_p\varphi_f/L_q, b_4 = 1/L_q, c_1 = -R_s/L_d, c_2 = L_q n_p/L_d, c_3 = 1/L_d$.

This study aims to devise a neuro-learning-based adaptive prescribed performance controller for PMSM system (2) to guarantee the following:

(a) The output signal $x_1$ follows the reference signal $x_d$ asymptotically

Table 1: The denotations of parameters for the PMSM.

| Parameters | Denotations | Units |
|---|---|---|
| $\theta$ | Rotor angular | rad |
| $\omega$ | Rotor angular velocity | rad/s |
| $i_q$ | $q$ − axis current | A |
| $i_d$ | $d$ − axis current | A |
| $u_q$ | $q$ − axis voltages | V |
| $u_d$ | $d$ − axis voltages | V |
| $n_p$ | Pole pairs | |
| $J$ | Rotor moment of inertia | $\mathrm{kg}\cdot\mathrm{m}^2$ |
| $B$ | Friction coefficient | N/(rad/s) |
| $\varphi_f$ | Magnet flux linkage of inertia | Wb |
| $R_S$ | Armature resistance | W |
| $x_{\mathrm{TL}}$ | Load torque | N · m |
| $L_d$ | $d$ − axis stator inductance | H |
| $L_q$ | $q$ − axis stator inductance | H |

(b) The tracking errors of all states are limited to the given boundaries

(c) The stability of the system is minimally affected by time delays, and the boundedness of all signals in the closed-loop system is guaranteed

To effectively implement our controller design, the following assumptions and lemmas are presented in advance.

**Lemma 1** (see [37]). *For arbitrary continuous function* $h(\zeta_1,\ldots,\zeta_n)$: $\mathbb{R}^{m_1}\times\cdots\times\mathbb{R}^{m_n}\longrightarrow\mathbb{R}$ *fulfilling* $h(0,\ldots,0)=0$, *in which* $\zeta_j\in\mathbb{R}^{m_j}$, $j=1,\ldots,n$, *there exist smooth-positive functions* $\varpi_j(\zeta_j)$: $\mathbb{R}^{m_j}\longrightarrow\mathbb{R}$ *such that* $|h(\zeta_1,\ldots,\zeta_n)|\le\sum_{j=1}^{n}\varpi_j(\zeta_j)$.

*Assumption 2* (see [38, 39]). The uncertain nonlinear time-delay functions $\chi_i(\cdot)$: $R^i\longrightarrow R\,(i=1,\cdots,n)$ satisfy the following inequalities:

$$\left|\chi_i\left(\overline{x}_i(t-\sigma_i)\right)\right|\le\vartheta_i\sum_{j=1}^{i}h_{\mathrm{ij}}\left(x_j\left(t-\sigma_j\right)\right),\tag{3}$$

where $h_{\mathrm{ij}}(\cdot)\,(i=1,\cdots,n,\ j=1,\cdots,n)$ are unknown positive-continuous functions and $\vartheta_i>0$.

*Remark 3.* According to Lemma 1, we know that if $h(\zeta_1,\ldots,\zeta_n)=\chi_i(\overline{x}_i(t-\sigma_i))$, then $|\chi_i(\overline{x}_i(t-\sigma_i))|\le\sum_{j=1}^{i}\varpi_j(x_j(t-\sigma_j))$. Because $\vartheta_i h_{\mathrm{ij}}(x_j(t-\sigma_j))$ are positive-continuous functions, we can choose the function $\varpi_j(\overline{x}_i(t-\sigma_i))$ as $\varpi_j(\overline{x}_i(t-\sigma_i))=\vartheta_i h_{ij}(x_j(t-\sigma_j))$. Therefore, combining with Lemma 1, we can conclude that the assumption of inequality (3) is reasonable. The same assumption can be seen in the work [38].

*Assumption 4* (see [40]). The reference signal $x_d$ and its n-order derivative $x_d^{(n)}$ are continuous and bounded.

**Lemma 5** (see [41]). *Given a nonlinear system* $\dot{x}=f(x)$, *if there exist a smooth-positive definite function* $V(x)$ *and some scalars* $a>0$, $b>0$ *fulfilling*

$$\dot{V}(x)\le-aV(x)+b,t\ge0,\tag{4}$$

*one can get that* $x(t)$ *is uniformly bounded.*

**Lemma 6** (see [42]). *For* $\forall(\wp,\varsigma)\in R^2$, *the relationship holds*

$$\wp\varsigma\le\frac{1}{\overline{p}}|\wp|^{\overline{p}}+\frac{1}{\overline{q}}|\varsigma|^{\overline{q}},\tag{5}$$

*in which* $\wp,\varsigma,\overline{p},\overline{q}$ *are real quantities and* $1/\overline{p}+1/\overline{q}=1$.

**Lemma 7** (see [43]). *If* $\Phi(Z)$: $R^q\longrightarrow R$ *is an unknown continuous function on a compact set* $\Omega_Z$, *there exists RBFNNs (seen in Figure 1) that* $\Phi(Z)$ *can be approximated by*

$$\Phi(Z)=\theta^T\psi(Z),\tag{6}$$

*where* $Z=[z_1,z_2,\cdots,z_q]\in R^q$ *is the input vector,* $\theta=[\theta_1,\theta_2,\ldots,\theta_l]^T\in R^l$ *is the ideal weight vector with the node* $l>0$, *and* $\psi(Z)=[\psi_1(Z),\psi_2(Z),\cdots,\psi_l(Z)]^T$ *is the basic function vector, and the Gaussian functions are adopted as the basic function*

$$\psi(Z)=\exp\left[-\frac{(Z-\mu_i)^T(Z-\mu_i)}{b_i^{\,2}}\right],\quad i=1,2,\cdots,l,\tag{7}$$

*where* $\mu_i=[\mu_{i1},\cdots,\mu_{iq}]^T$ *is the center of the receptive field and* $b_i$ *is the width of the Gaussian function. By installing lots of hidden neurons as* $\Phi(Z)=\theta^{*T}\Phi(Z)+\delta$, $\Phi(Z)$ *can be approximated online with any precision via RBFNNs, in which the error* $\delta$ *can be tuned very small by adopting the ideal weight vector* $\theta^*=[\theta_1^*,\theta_2^*,\ldots,\theta_l^*]^T$ *as*

$$\theta^*:=\arg\quad\min_{W\in R^l}\left\{\sup_{X\in\Omega_X}\left|\Phi(Z)-\theta^{*T}\psi(Z)\right|\right\}.\tag{8}$$

*Remark 8.* Noting that there are unknown-nonlinear functions within (2), which hinder the controller design, the authors in [44] show that neural networks can evaluate nonlinear functions with arbitrary precision. Due to the advantages of simple structure and good approximation ability, this study introduces RBFNNs to deal with nonlinear functions.

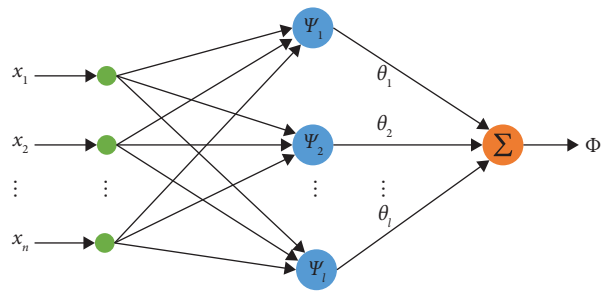


Figure 1: The structure of RBFNN.

Then, define

$$\Theta_i = \left\|\theta_i^*\right\|^2, \tag{9}$$

where $\|\theta_i^*\|$ is the norm of $\theta_i$.

Let $\hat{\Theta}_i$ be the estimate of the $\Theta_i$. Then, the corresponding estimation error is $\tilde{\Theta}_i = \Theta_i - \hat{\Theta}_i$ and $\dot{\tilde{\Theta}}_i = -\dot{\hat{\Theta}}_i$.

*Remark 9.* In order to save computational resources and obtain a relatively simple controller, we estimate the squared value of the weight norm of RBFNNs.

## 3. The Control Design

*3.1. The Full-State Prescribed Performance.* The error surfaces are defined as

$$\begin{cases} e_1 = x_1 - x_d, \\ e_i = x_i - \overline{\alpha}_{i-1}, \quad i = 2, 3, \\ e_4 = x_4, \end{cases} \tag{10}$$

where the variables $\overline{\alpha}_{i-1}$ are given later.

To achieve full-state prescribed performance control, the errors in (10) are constrained strictly in the predefined domains as

$$-\underline{\delta}\,\nu(t) \le e_i \le \overline{\delta}\nu(t), \quad i = 1, \cdots, 4, \tag{11}$$

where $\overline{\delta}, \underline{\delta}$ are positive constants that can adjust the upper and lower bounds.

Unlike the traditional PPC in references [35, 36, 38], a new prescribed performance function is constructed as

$$\nu_i(t) = (\nu_{i0} - \nu_{i\infty})(\kappa_i t + e)^{-\rho t} + \nu_{i\infty} + \ell_2 \tan h\left(\ell_3 \dot{\overline{x}}_{\mathrm{TL}}^{\,2}\right), \tag{12}$$

in which $\overline{x}_{\mathrm{TL}}$ is a continuous function about external varying loads and $\rho, \kappa_i, \nu_{i0}, \nu_{i\infty}, \ell_2, \ell_3$ are positive constants. When there is no external load disturbance, i.e., $\dot{\overline{x}}_{\mathrm{TL}} = 0$, the maximum overshoots of $e_i(t)$ are limited in the sets $(\overline{\delta}\nu_{i0}, \underline{\delta}\,\nu_{i0})$, and the maximum permissible ranges of $e_i(t)$ at the stable state are the interval $(-\overline{\delta}\nu_{i\infty}, \underline{\delta}\,\nu_{i\infty})$.

*Remark 10.* We have improved the traditional PPC in [35, 36, 38], in which the performance function is chosen as

$$\nu(t) = (\nu_0 - \nu_\infty)e^{-\rho t} + \nu_\infty. \tag{13}$$

First, the terms $(\kappa_i t + e)^{-\rho t}$ are designed to enhance the convergence rate greatly by tuning the positive parameters $\kappa_i$. Then, the influences of external load perturbations on the prescribed performance of PMSM are considered, and an adaptive compensated term $\ell_2 \tan h(\ell_3 \dot{\overline{x}}_{\mathrm{TL}}^{\,2})$ is constructed to resist the load oscillations by adjusting the predefined boundaries automatically. Therefore, the designed performance function has a wider application value.

Subsequently, let us define the coordinate transformations as

$$\mathfrak{T}_i = \frac{1}{2}\ln\left(\frac{\overline{\delta} + e_i/\nu_i}{\underline{\delta} - e_i/\nu_i}\right), \quad i = 1, \cdots, 4, \tag{14}$$

where the error convert functions $\mathfrak{T}_i$ depend entirely on the variables $e_i/\nu_i$.

The derivatives of $\mathfrak{T}_i$ are

$$\dot{\mathfrak{T}}_i = \lambda_i\left(\dot{e}_i - \frac{e_i}{\nu_i}\dot{\nu}_i\right), \tag{15}$$

where

$$\lambda_i = \frac{1}{2}\left(\frac{1}{\nu_i\overline{\delta} + e_i} - \frac{1}{\nu_i\,\underline{\delta} - e_i}\right). \tag{16}$$

*Remark 11.* From (11), we know that the inequalities $-\underline{\delta} < e_i/\nu_i < \overline{\delta}$ hold. Based on (14), the value domains of variables $\mathfrak{T}_i$ are $(-\infty, +\infty)$. Thus, the constrained problems are transformed into equivalent nonconstrained ones. In the controller design, if we ensure that $\mathfrak{T}_i \in R$ are bounded, the error constraints (11) will always hold.

*3.2. The Time-Varying Filters.* Define the time-varying filters and the filter errors as

$$\varpi_i e^{-\beta t}\dot{\overline{\alpha}}_i + \overline{\alpha}_i = \alpha_i, \overline{\alpha}_i(0) = \alpha_i(0), \quad i = 1, 2, \tag{17}$$

$$\Upsilon_i = \overline{\alpha}_i - \alpha_i, \quad i = 1, 2, \tag{18}$$

where $\alpha_i$ are the inputs of the filters which are the virtual control laws given later, the variables $\overline{\alpha}_i$ are outputs, and $\varpi_i, \beta$ are the positive design constants.

**Lemma 12.** *The filters (17) are low-pass, and the filtering errors (18) converge asymptotically to zero.*

*Proof.* First, we analyze the filtering characteristics of the proposed filter from the s-domain. Applying the Laplace transform to the equation (17), one gets

$$\varpi_i(s + \beta)\overline{\alpha}_i(s) + \overline{\alpha}_i(s) = \alpha_i(s), \tag{19}$$

where $s = j\omega + \sigma$.

Thus,

$$\frac{\overline{\alpha}_i(s)}{\alpha_i(s)} = \frac{1}{\varpi_i(s + \beta) + 1}. \tag{20}$$

From (20), we know that the filters work when $s \longrightarrow 0$. When $s \longrightarrow \infty$, the filters are disabled.

Then, by combining (17) with (18), we have

$$\Upsilon_i = -\varpi_i e^{-\beta t}\dot{\bar{\alpha}}_i. \tag{21}$$

As a result, we get $\lim_{t\longrightarrow\infty}\Upsilon_i = 0$.

According to the above analysis, we have completed the proof of Lemma 6. □

*Remark 13.* Compared with the conventional first-order filter [3], the proposed time-varying filters enable faster filtering, and the tracking error is asymptotically converged to zero.

*3.3. The Backstepping Controller Design.* In this section, by integrating the dynamic surface method and RBFNNs into the backstepping framework, we have constructed the full-state prescribed performance control scheme for the PMSM with time delays. The framework of the controller is shown in Figure 2.

*Step 14.* Select the candidate Lyapunov function as

$$V_1 = \frac{1}{2}\mathfrak{I}_1{}^2 + \frac{1}{2\eta_1}\tilde{\Theta}_1{}^2 + \mathbb{Z}_1, \tag{22}$$

where $\eta_1 > 0$ and $\mathbb{Z}_1 = \vartheta_1{}^2\int_{t-\sigma_1}^{t} h_{11}{}^2(x_1(\sigma))\mathrm{d}\sigma$.

Calculating the time derivative of $V_1$ leads to

$$\dot{V}_1 = \mathfrak{I}_1\dot{\mathfrak{I}}_1 - \frac{1}{\eta_1}\tilde{\Theta}_1\dot{\hat{\Theta}}_1 + \vartheta_1^2\, h_{11}^2\ (x_1(t)) - \vartheta_1^2\, h_{11}^2\ (x_1(t-\sigma_1)). \tag{23}$$

Based on (10) and (18), one has

$$\dot{e}_1 = e_2 + \Upsilon_1 + \alpha_1 + \chi_1(x_1(t-\sigma_1)) - \dot{x}_d. \tag{24}$$

Combining (15) with (24), we obtain

$$\dot{\mathfrak{I}}_1 = \lambda_1\left(e_2 + \Upsilon_1 + \alpha_1 + \chi_1(x_1(t-\sigma_1)) - \dot{x}_d - \frac{e_1}{\nu_1}\dot{\nu}_1\right). \tag{25}$$

Substituting (25) into (23) generates

$$\dot{V}_1 = \lambda_1\mathfrak{I}_1\left(e_2 + \Upsilon_1 + \alpha_1 + \chi_1(\bar{x}_1(t-\sigma_1)) - \dot{x}_d - \frac{e_1}{\nu_1}\dot{\nu}_1\right) - \frac{1}{\eta_1}\tilde{\Theta}_1\dot{\hat{\Theta}}_1 + \vartheta_1^2\, h_{11}^2\ (x_1(t)) - \vartheta_1^2\, h_{11}^2\ (x_1(t-\sigma_1)). \tag{26}$$

According to (3) and Young's inequality, we obtain

$$\begin{cases} \mathfrak{I}_1\lambda_1\chi_1(\bar{x}_1(t-\sigma_1)) \le \dfrac{1}{4}(\mathfrak{I}_1\lambda_1)^2 + \vartheta_1^2\, h_{11}^2\ (x_1(t-\sigma_1)), \\ \lambda_1\mathfrak{I}_1 e_2 \le \dfrac{1}{2}(\lambda_1\mathfrak{I}_1)^2 + \dfrac{1}{2}e_2^2, \\ \lambda_1\mathfrak{I}_1\Upsilon_1 \le \dfrac{1}{2}(\lambda_1\mathfrak{I}_1)^2 + \dfrac{1}{2}\Upsilon_1^2. \end{cases} \tag{27}$$

Substituting (27) into (26) yields

$$\dot{V}_1 \le \lambda_1\mathfrak{I}_1\left(\alpha_1 - \dot{x}_d - \frac{e_1}{\nu_1}\dot{\nu}_1\right) + \frac{5}{4}(\lambda_1\mathfrak{I}_1)^2 + \frac{1}{2}\Upsilon_1^2 + \frac{1}{2}e_2{}^2 - \frac{1}{\eta_1}\tilde{\Theta}_1\dot{\hat{\Theta}}_1 + \vartheta_1^2 h_{11}^2(x_1(t)). \tag{28}$$

Define the nonlinear function $\Phi_1(Z_1)$ as

$$\Phi_1(Z_1) = \frac{1}{\mathfrak{I}_1\lambda_1}H_1 + \frac{1}{\mathfrak{I}_1\lambda_1}G_1, \tag{29}$$

where $Z_1 = [x_1, \mathfrak{I}_1, \lambda_1]^T$, $H_1 = \vartheta_1^2 h_{11}^2(x_1(t))$, $G_1 = \vartheta_1^2\int_{t-\tau}^{t} h_{11}^2(x_1(\sigma))\mathrm{d}\sigma$, and $\sigma_1 \le \tau$.

Then, (28) becomes

$$\dot{V}_1 \le \mathfrak{I}_1\lambda_1\Phi_1(Z_1) + \mathfrak{I}_1\lambda_1\left(\alpha_1 - \dot{x}_d - \frac{e_1}{\nu_1}\dot{\nu}_1\right) + \frac{5}{4}(\mathfrak{I}_1\lambda_1)^2 + \frac{1}{2}\Upsilon_1^2 + \frac{1}{2}e_2{}^2 - G_1 - \frac{1}{\eta_1}\tilde{\Theta}_1\dot{\hat{\Theta}}_1. \tag{30}$$

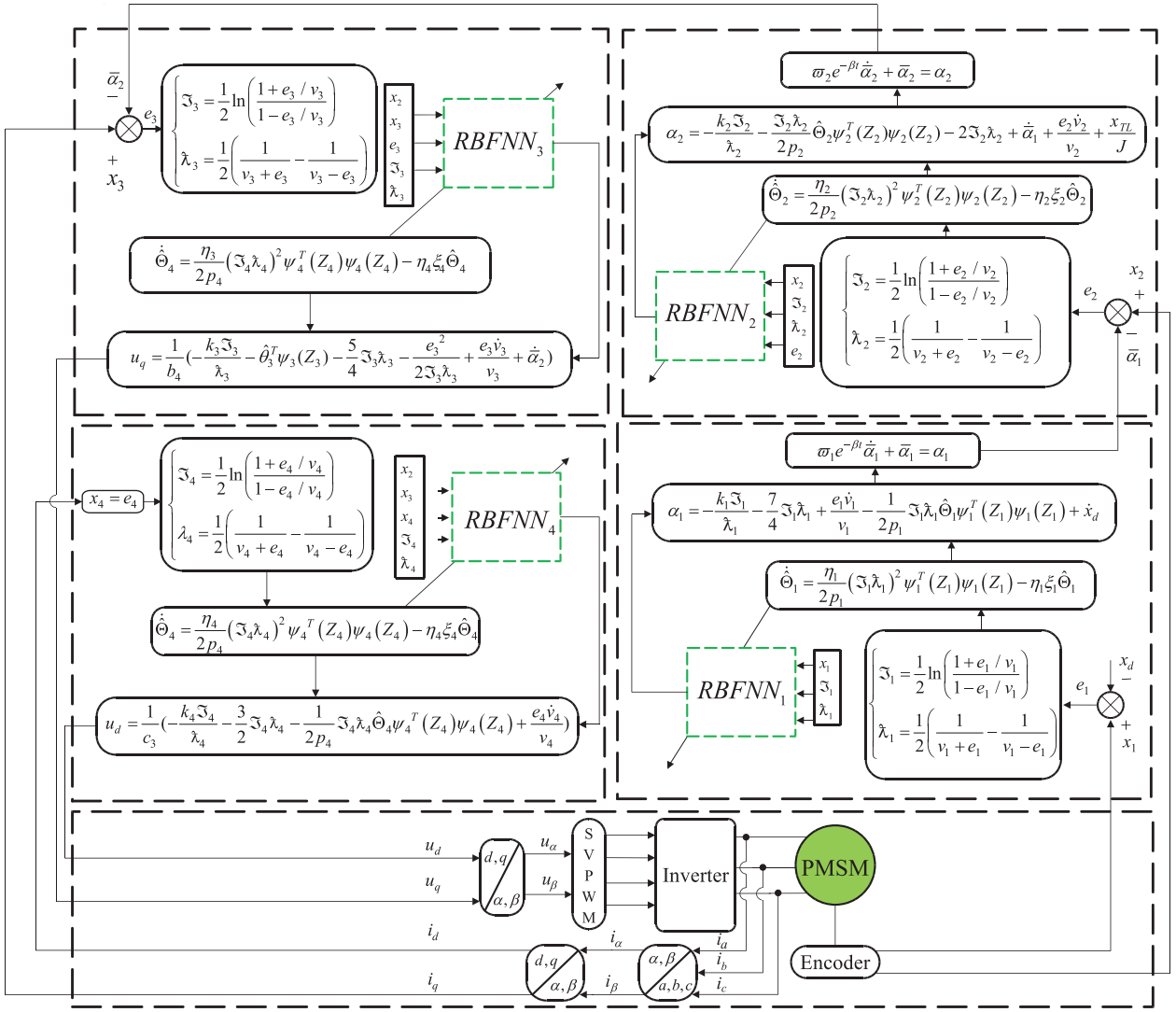


Figure 2: Overview of the control framework for the PMSM.

From (29), we know that $\Phi_1(Z_1)$ is an unknown continuous function on the compact set $\Omega_{Z_1}$. Based on Lemma 7, it can be approximated as

$$\Phi_1(Z_1) = \theta_1^{*T}\psi_1(Z_1) + \delta_1(Z_1), \left|\delta_1(Z_1)\right| \le \bar{\delta}_1. \tag{31}$$

Via Young's inequality, we get

$$\begin{aligned}\mathfrak{I}_1\lambda_1\left(\theta_1^{*T}\psi_1(Z_1) + \delta_1(Z_1)\right) &\le \left|\mathfrak{I}_1\lambda_1\right|\left(\left\|\theta_1^*\right\|\left\|\psi_1(Z_1)\right\| + \bar{\delta}_1\right)\\ &\le \frac{1}{2p_1}\left(\mathfrak{I}_1\lambda_1\right)^2\Theta_1\psi_1^T(Z_1)\psi_1(Z_1) + \frac{p_1}{2} + \frac{1}{2}\left(\mathfrak{I}_1\lambda_1\right)^2 + \frac{1}{2}\bar{\delta}_1^2,\end{aligned} \tag{32}$$

where $p_1$ is a positive constant.

Taking (31) and (32) into (30) generates

$$\dot{V}_1 \le \mathfrak{F}_1 \lambda_1 \left( \alpha_1 - \dot{x}_d - \frac{e_1}{\nu_1} \dot{\nu}_1 \right) + \frac{1}{2p_1} (\mathfrak{F}_1 \lambda_1)^2 \Theta_1 {\psi_1}^T (Z_1) \psi_1 (Z_1) + \frac{7}{4} (\mathfrak{F}_1 \lambda_1)^2 - \frac{1}{\eta_1} \tilde{\Theta}_1 \dot{\hat{\Theta}}_1 + \frac{1}{2} {e_2}^2 + \frac{1}{2} \left( {\Upsilon_1}^2 + p_1 + {\bar{\delta}_1}^2 \right) - G_1. \tag{33}$$

Construct the adaptive law $\dot{\hat{\Theta}}_1$ and the virtual control law $\alpha_1$ as

$$\dot{\hat{\Theta}}_1 = \frac{\eta_1}{2p_1} (\mathfrak{F}_1 \lambda_1)^2 {\psi_1}^T (Z_1) \psi_1 (Z_1) - \eta_1 \xi_1 \hat{\Theta}_1, \tag{34}$$

$$\alpha_1 = -\frac{k_1 \mathfrak{F}_1}{\lambda_1} - \frac{7}{4} \mathfrak{F}_1 \lambda_1 - \frac{1}{2p_1} \mathfrak{F}_1 \lambda_1 \hat{\Theta}_1 {\psi_1}^T (Z_1) \psi_1 (Z_1) + \frac{e_1 \dot{\nu}_1}{\nu_1} + \dot{x}_d, \tag{35}$$

where $k_1, \xi_1$ are positive constants.

Substituting (34) and (35) into (33) produces

$$\dot{V}_1 \le -k_1 {\mathfrak{F}_1}^2 + \frac{1}{2} \Upsilon_1^2 + \xi_1 \tilde{\Theta}_1 \hat{\Theta}_1 + \frac{1}{2} e_2^2 + \frac{1}{2} \bar{\delta}_1^2 + \frac{1}{2} p_1 - G_1. \tag{36}$$

Combining the definition of $\hat{\Theta}_1$ with Young's inequality, one obtains

$$\tilde{\Theta}_1 \hat{\Theta}_1 = \tilde{\Theta}_1 \left( \Theta_1 - \tilde{\Theta}_1 \right) \le -\frac{1}{2} \tilde{\Theta}_1^2 + \frac{1}{2} \Theta_1^2. \tag{37}$$

Inserting (37) into (36) yields

$$\dot{V}_1 \le -k_1 {\mathfrak{F}_1}^2 - \frac{1}{2} \xi_1 \tilde{\Theta}_{11}^2 - G_1 + \frac{1}{2} \Upsilon_1^2 + \frac{1}{2} \xi_1 \Theta_1^2 + \frac{1}{2} {e_2}^2 + \frac{1}{2} \bar{\delta}_1^2 + \frac{1}{2} p_1. \tag{38}$$

*Step 2.* The candidate Lyapunov function is designed as

$$V_2 = V_1 + \frac{1}{2} \mathfrak{F}_2^2 + \frac{1}{2\eta_2} \tilde{\Theta}_2^2 + \mathbb{Z}_2, \tag{39}$$

where $\mathbb{Z}_2 = {\vartheta_2}^2 \sum_{j=1}^{2} \int_{t-\sigma_j}^{t} {h_{2j}}^2 (x_j(\sigma)) \mathrm{d}\sigma$ and $\eta_2 > 0$.

The time derivative of $V_2$ is

$$\dot{V}_2 = \dot{V}_1 + \mathfrak{F}_2 \dot{\mathfrak{F}}_2 - \frac{1}{\eta_2} \tilde{\Theta}_2 \dot{\hat{\Theta}}_2 + \vartheta_2^2 \sum_{j=1}^{2} {h_{2j}}^2 (x_2(t)) - \vartheta_2^2 \sum_{j=1}^{2} {h_{2j}}^2 \left( x_j \left( t - \sigma_j \right) \right). \tag{40}$$

Integrating (10) and (18) and the second equation of (2), we have

$$\dot{e}_2 = a_1 x_2 + (a_2 - 1) x_3 + a_3 x_3 x_4 - \frac{x_{\mathrm{TL}}}{J} + \chi_2 \left( \bar{x}_2 \left( t - \sigma_2 \right) \right) + e_3 + \Upsilon_2 + \alpha_2 - \dot{\bar{\alpha}}_1. \tag{41}$$

Fusing (15) and (41) into (40) yields

$$\dot{V}_2 = \dot{V}_1 - \frac{1}{\eta_2}\tilde{\Theta}_2\dot{\hat{\Theta}}_2 + \vartheta_2^2\sum_{j=1}^{2} h_{2j}{}^2(x_2(t)) - \vartheta_2^2\sum_{j=1}^{2} h_{2j}{}^2\left(x_j\left(t-\sigma_j\right)\right) + \mathfrak{T}_2\lambda_2\left(a_1x_2 + (a_2-1)x_3 + a_3x_3x_4 - \frac{x_{\mathrm{TL}}}{J} + \chi_2(\bar{x}_2(t-\sigma_2)) + e_3 + \Upsilon_2 + \alpha_2 - \dot{\bar{\alpha}}_1 - \frac{e_2\dot{\nu}_2}{\nu_2{}^2}\right). \tag{42}$$

Based on (3) and Young's inequality,

$$\begin{cases} \mathfrak{T}_2\lambda_2\chi_2(\bar{x}_2(t-\sigma_2)) \le \frac{1}{2}(\mathfrak{T}_2\lambda_2)^2 + \vartheta_2^2\sum_{j=1}^{2} h_{2j}{}^2\left(x_j\left(t-\sigma_j\right)\right), \\ \mathfrak{T}_2\lambda_2 e_3 \le \frac{1}{2}(\mathfrak{T}_2\lambda_2)^2 + \frac{1}{2}e_3^2, \\ \mathfrak{T}_2\lambda_2\Upsilon_2 \le \frac{1}{2}(\mathfrak{T}_2\lambda_2)^2 + \frac{1}{2}\Upsilon_2^2. \end{cases} \tag{43}$$

Inserting (43) into (42) results in

$$\dot{V}_2 \le \dot{V}_1 + \mathfrak{T}_2\lambda_2\left(a_1x_2 + (a_2-1)x_3 + a_3x_3x_4 - \frac{x_{\mathrm{TL}}}{J} + \alpha_2 - \dot{\bar{\alpha}}_1 - \frac{e_2\dot{\nu}_2}{\nu_2}\right) + \frac{e_3{}^2}{2} + \frac{\Upsilon_2{}^2}{2} - \frac{1}{\eta_2}\tilde{\Theta}_2\dot{\hat{\Theta}}_2 + \frac{3}{2}(\mathfrak{T}_2\lambda_2)^2 + \vartheta_2^2\sum_{j=1}^{2} h_{2j}{}^2(x_2(t)). \tag{44}$$

Construct the function $\Phi_2(Z_2)$ as

$$\Phi_2(Z_2) = a_1x_2 - \frac{1}{2\mathfrak{T}_2\lambda_2}e_2^2 + \frac{H_2}{\mathfrak{T}_2\lambda_2} + \frac{1}{\mathfrak{T}_2\lambda_2}G_2, \tag{45}$$

where $Z_2 = [x_2, \mathfrak{T}_2, \lambda_2, e_2]^T$, $G_2 = \vartheta_2{}^2\sum_{j=1}^{2}\int_{t-\tau}^{t} h_{2j}{}^2(x_j(\sigma))\mathrm{d}\sigma$, and $H_2 = \vartheta_2{}^2\sum_{j=1}^{2} h_{2j}{}^2(x_2(t))$.

Thus, (44) can be rewritten as

$$\dot{V}_2 \le \dot{V}_1 + \mathfrak{T}_2\lambda_2\Phi(Z_2) - \frac{1}{\eta_2}\tilde{\Theta}_2\dot{\hat{\Theta}}_2 + \mathfrak{T}_2\lambda_2\left(\alpha_2 - \dot{\bar{\alpha}}_1 - \frac{e_2\dot{\nu}_2}{\nu_2} - \frac{x_{TL}}{J}\right) + \mathfrak{T}_2\lambda_2\left(\frac{a_1}{J} - 1\right)x_3 + \mathfrak{T}_2\lambda_2\frac{a_2x_3x_4}{J} + \frac{3}{2}(\mathfrak{T}_2\lambda_2)^2 - \frac{1}{2}e_2^2 + \frac{1}{2}e_2^3 + \frac{1}{2}\Upsilon_2^2 - G_2. \tag{46}$$

From (45), we know that $\Phi_2(Z_2)$ is a continuous nonlinear function on the compact set $\Omega_{Z_2}$. Similarly, based on Lemma 7, we can approximate it as

$$\Phi_2(Z_2) = \theta_2{}^{*T}\psi_2(Z_2) + \delta_2(Z_2), \left|\delta_2(Z_2)\right| \le \bar{\delta}_2. \tag{47}$$

Like (32), we have

$$\mathfrak{T}_2\lambda_2\left(\theta_2{}^{*T}\psi_2(Z_2) + \delta_2(Z_2)\right) \le \frac{1}{2p_2}(\mathfrak{T}_2\lambda_2)^2\Theta_2\psi_2{}^T(Z_2)\psi_2(Z_2) + \frac{p_2}{2} + \frac{1}{2}(\mathfrak{T}_2\lambda_2)^2 + \frac{1}{2}\bar{\delta}_2^2, \tag{48}$$

where $p_2$ is a positive design constant.

Substituting (47) and (48) into (46) leads to

$$\dot{V}_2 \le \dot{V}_1 + \frac{1}{2p_2}(\mathfrak{F}_2 \text{ƛ}_2)^2 \Theta_2 \psi_2^{\ T}(Z_2)\psi_2(Z_2) + \mathfrak{F}_2 \text{ƛ}_2\left(\alpha_2 - \dot{\bar{\alpha}}_1 - \frac{e_2\dot{\nu}_2}{\nu_2} - \frac{x_{TL}}{J}\right)$$
$$- G_2 + 2(\mathfrak{F}_2 \text{ƛ}_2)^2 - \frac{1}{\eta_2}\tilde{\Theta}_2\dot{\hat{\Theta}}_2 + \frac{1}{2}\bar{\delta}_2^{\ 2} - \frac{1}{2}e_2^{\ 2} + \frac{1}{2}e_3^{\ 2}$$
$$+ \frac{1}{2}\Upsilon_2^{\ 2} + \mathfrak{F}_2 \text{ƛ}_2\left(\left(\frac{a_1}{J} - 1\right)x_3 + \frac{a_2 x_3 x_4}{J}\right) + \frac{1}{2}p_2. \tag{49}$$

Then, construct the adaptive law $\dot{\hat{\Theta}}_2$ and the virtual control law $\alpha_2$ as

$$\dot{\hat{\Theta}}_2 = \frac{\eta_2}{2p_2}(\mathfrak{F}_2 \text{ƛ}_2)^2 \psi_2^{\ T}(Z_2)\psi_2(Z_2) - \eta_2 \xi_2 \hat{\Theta}_2, \tag{50}$$

$$\alpha_2 = -\frac{k_2 \mathfrak{F}_2}{\text{ƛ}_2} - 2\mathfrak{F}_2 \text{ƛ}_2 - \frac{1}{2p_2}(\mathfrak{F}_2 \text{ƛ}_2)\hat{\Theta}_2 \psi_2^{\ T}(Z_2)\psi_2(Z_2) + \dot{\bar{\alpha}}_1 + \frac{e_2\dot{\nu}_2}{\nu_2} + \frac{x_{\mathrm{TL}}}{J}, \tag{51}$$

where $\xi_2, k_2$ are positive constants.

Integrating (50) and (51) into (49) gets

$$\dot{V}_2 \le \dot{V}_1 - \frac{k_2 \mathfrak{F}_2}{\text{ƛ}_2} - \frac{e_2^2}{2\mathfrak{F}_2 \text{ƛ}_2} - G_2 + \xi_2 \tilde{\Theta}_2 \hat{\Theta}_2 + \frac{1}{2}\bar{\delta}_2^{\ 2} + \frac{1}{2}p_2$$
$$- \frac{1}{2}e_2^{\ 2} + \frac{1}{2}e_3^{\ 2} + \frac{1}{2}\Upsilon_2^{\ 2} + \mathfrak{F}_2 \text{ƛ}_2\left(\left(\frac{a_1}{J} - 1\right)x_3 + \frac{a_2 x_3 x_4}{J}\right). \tag{52}$$

Similar to (37), we can obtain

$$\tilde{\Theta}_2 \hat{\Theta}_2 \le -\frac{1}{2}\tilde{\Theta}_2^{\ 2} + \frac{1}{2}\Theta_2^{\ 2}. \tag{53}$$

Fusing (38) and (53) into (52) generates

$$\dot{V}_2 \le -\sum_{i=1}^{2} k_i \mathfrak{F}_i^{\ 2} - \frac{1}{2}\sum_{i=1}^{2}\tilde{\Theta}_2^{\ 2} - \sum_{i=1}^{2} G_i + \frac{1}{2}\sum_{i=1}^{2}\Upsilon_i^{\ 2} + \frac{1}{2}\sum_{i=1}^{2}\xi_i \Theta_2^{\ 2}$$
$$+ \frac{1}{2}\sum_{i=1}^{2} p_i + \frac{1}{2}\sum_{i=1}^{2}\bar{\delta}_i^{\ 2} + \frac{1}{2}e_3^{\ 2} + \mathrm{s}\mathfrak{F}_2 \text{ƛ}_2\left(\left(\frac{a_1}{J} - 1\right)x_3 + \frac{a_2 x_3 x_4}{J}\right). \tag{54}$$

*Step 15.* Adopt the candidate Lyapunov function as

$$V_3 = V_2 + \frac{1}{2}\mathfrak{F}_3^{\ 2} + \frac{1}{2\eta_3}\tilde{\Theta}_3^{\ 2} + \mathbb{Z}_3, \tag{55}$$

where $\mathbb{Z}_3 = \vartheta_3^{\ 2}\sum_{j=1}^{3}\int_{t-\sigma_j}^{t} h_{3j}^{\ 2}(x_j(\sigma))\mathrm{d}\sigma$ and $\eta_3$ is a positive constant to be designed.

Then,

$$\dot{V}_3 = \dot{V}_2 + \mathfrak{F}_3\dot{\mathfrak{F}}_3 - \frac{1}{\eta_3}\tilde{\Theta}_3\dot{\hat{\Theta}}_3 + \vartheta_3^{\ 2}\sum_{j=1}^{3} h_{3j}^{\ 2}\left(x_j(t)\right) - \vartheta_3^2\sum_{j=1}^{3} h_{3j}^{\ 2}\left(x_j\left(t-\sigma_j\right)\right). \tag{56}$$

Based on (10) and (18) and the third equation of (2), one gets

$$\dot{e}_3 = b_1 x_3 + b_2 x_2 x_4 + b_3 x_2 + b_4 u_q + \chi_3(\bar{x}_3(t-\sigma_3)) - \dot{\bar{\alpha}}_2. \tag{57}$$

Substituting (15) and (57) into (56) yields

$$\dot{V}_3 = \dot{V}_2 + \mathfrak{I}_3\lambda_3\left(b_1x_3 + b_2x_2x_4 + b_3x_2 + b_4u_q + \chi_3\left(\overline{x}_3\left(t-\sigma_3\right)\right) - \dot{\overline{\alpha}}_2 - \frac{e_3\dot{\nu}_3}{\nu_3}\right) - \frac{1}{\eta_3}\tilde{\Theta}_3\dot{\hat{\Theta}}_3 + \vartheta_3{}^2\sum_{j=1}^{3}h_{3j}{}^2\left(x_j(t)\right) - \vartheta_3{}^2\sum_{j=1}^{3}h_{3j}{}^2\left(x_j\left(t-\sigma_j\right)\right). \tag{58}$$

Combining (3) with Young's inequality, we have

$$\mathfrak{I}_3\lambda_3\chi_3\left(\overline{x}_3\left(t-\sigma_3\right)\right) \le \frac{3}{4}\left(\mathfrak{I}_3\lambda_3\right)^2 + \vartheta_3{}^2\sum_{j=1}^{3}h_{3j}{}^2\left(x_j\left(t-\sigma_3\right)\right). \tag{59}$$

Inserting (59) into (58) leads to

$$\dot{V}_3 \le \dot{V}_2 + \mathfrak{I}_3\lambda_3\left(b_1x_3 + b_2x_2x_4 + b_3x_2 + b_4u_q - \dot{\overline{\alpha}}_2 - \frac{e_3\dot{\nu}_3}{\nu_3}\right) - \frac{1}{\eta_3}\tilde{\Theta}_3\dot{\hat{\Theta}}_3 + \frac{3}{4}\left(\mathfrak{I}_3\lambda_3\right)^2 + \vartheta_3{}^2\sum_{j=1}^{3}h_{3j}{}^2\left(x_j(t)\right). \tag{60}$$

Define the function $\Phi_3(Z_3)$ as

$$\Phi_3\left(Z_3\right) = b_1x_3 + b_3x_2 + \frac{e_3{}^2}{2\mathfrak{I}_3\lambda_3} + \frac{H_3}{\mathfrak{I}_3\lambda_3} + \frac{G_3}{\mathfrak{I}_3\lambda_3}, \tag{61}$$

where $Z_3 = [x_2, x_3, e_3, \mathfrak{I}_3, \lambda_3]^T$, $G_3 = \vartheta_3{}^2\sum_{j=1}^{3}\int_{t-\tau}^{t}h_{3j}{}^2(x_j(\sigma))\mathrm{d}\sigma$, and $H_3 = \vartheta_3{}^2\sum_{j=1}^{3}h_{3j}{}^2(x_j(t))$.

Therefore, (60) becomes

$$\dot{V}_3 \le \dot{V}_2 + \mathfrak{I}_3\lambda_3\Phi_3\left(Z_3\right) + b_2\mathfrak{I}_3\lambda_3x_2x_4 + \frac{3}{4}\left(\mathfrak{I}_3\lambda_3\right)^2 + \mathfrak{I}_3\lambda_3b_4u_q - \frac{1}{\eta_3}\tilde{\Theta}_3\dot{\hat{\Theta}}_3 - G_3. \tag{62}$$

From (61), $\Phi_3(Z_3)$ is a continuous function on the compact set $\Omega_{Z_3}$. Thereby, based on Lemma 7, $\Phi_3(Z_3)$ can be approximated as

$$\Phi_3\left(Z_3\right) = \theta_3{}^{*T}\psi_3\left(Z_3\right) + \delta_3\left(Z_3\right), \left|\delta_3\left(Z_3\right)\right| \le \overline{\delta}_3. \tag{63}$$

By Young's inequality, we obtain

$$\mathfrak{I}_3\lambda_3\left(\theta_3{}^{*T}\psi_3\left(Z_3\right) + \delta_3\left(Z_3\right)\right) \le \frac{1}{2p_3}\left(\mathfrak{I}_3\lambda_3\right)^2\Theta_3\psi_3{}^T\left(Z_3\right)\psi_3\left(Z_3\right) + \frac{p_3}{2} + \frac{1}{2}\left(\mathfrak{I}_3\lambda_3\right)^2 + \frac{1}{2}\overline{\delta}_3, \tag{64}$$

where $p_3$ is a positive constant to be designed.

Bringing (63) and (64) into (62) yields

$$\dot{V}_3 \le \dot{V}_2 + \frac{5}{4}\left(\mathfrak{I}_3\lambda_3\right)^2 + \frac{1}{2p_3}\left(\mathfrak{I}_3\lambda_3\right)^2\Theta_3\psi_3{}^T\left(Z_3\right)\psi_3\left(Z_3\right) + \frac{9}{4}\left(\mathfrak{I}_3\lambda_3\right)^2 + \mathfrak{I}_3\lambda_3b_4u_q - \frac{1}{\eta_3}\tilde{\Theta}_3\dot{\hat{\Theta}}_3 + \frac{1}{2}\overline{\delta}_3{}^2 - G_3 - \frac{e_3{}^2}{2}. \tag{65}$$

Next, design the adaptive law $\dot{\hat{\Theta}}_3$ and the actual control $u_q$ as

$$\dot{\hat{\Theta}}_3 = \frac{\eta_3}{2p_3}(\mathfrak{F}_3\lambda_3)^2\psi_3^T(Z_3)\psi_3(Z_3) - \eta_3\xi_3\hat{\Theta}_3, \tag{66}$$

$$u_q = \frac{1}{b_4}\left(-\frac{k_3\mathfrak{F}_3}{\lambda_3} - \hat{\theta}_3^T\psi_3(Z_3) - \frac{5}{4}\mathfrak{F}_3\lambda_3 + \frac{e_3\dot{\nu}_3}{\nu_3} + \dot{\bar{\alpha}}_2\right), \tag{67}$$

where $\xi_3, k_3$ are positive constants.

Taking (66) and (67) into (65) generates

$$\dot{V}_3 \le \dot{V}_2 + \xi_3\tilde{\Theta}_3\hat{\Theta}_3 + \frac{\bar{\delta}_3^2}{2} + \frac{1}{2}p_3 - \frac{e_3^2}{2} - G_3 + b_2\mathfrak{F}_3\lambda_3x_2x_4. \tag{68}$$

Similar to (37), we have

$$\tilde{\Theta}_3\hat{\Theta}_3 \le -\frac{1}{2}\tilde{\Theta}_3^2 + \frac{1}{2}\Theta_3^2. \tag{69}$$

Substituting (54) and (69) into (68) obtains

$$\begin{aligned}\dot{V}_3 \le &-\sum_{i=1}^{3}k_i\mathfrak{F}_i^2 - \sum_{i=1}^{3}\frac{1}{2}\tilde{\Theta}_3^2 + \frac{1}{2}\sum_{i=1}^{3}\xi_i\Theta_3^2 - \sum_{i=1}^{3}G_i + \sum_{i=1}^{2}\frac{1}{2}\Upsilon_i^2\\ &+\frac{1}{2}\sum_{i=1}^{3}\bar{\delta}_i^2 + \frac{1}{2}\sum_{i=1}^{3}p_i + b_2\mathfrak{F}_3\lambda_3x_2x_4 + \mathfrak{F}_2\lambda_2\left(\left(\frac{a_1}{J} - 1\right)x_3 + \frac{a_2x_3x_4}{J}\right).\end{aligned} \tag{70}$$

*Step 16.* The candidate Lyapunov function is constructed as

$$V_4 = V_3 + \frac{1}{2}\mathfrak{F}_4^2 + \frac{1}{2\eta_4}\tilde{\Theta}_4^2 + \mathbb{Z}_4, \tag{71}$$

where $\mathbb{Z}_4 = \vartheta_4^2\sum_{J=1}^{4}\int_{t-\sigma_j}^{t}h_{4j}^2(x_j(\sigma))\mathrm{d}\sigma$ and $\eta_4$ is a positive constant.

The time derivative of $V_4$ can be indicated as

$$\dot{V}_4 = \dot{V}_3 + \mathfrak{F}_4\dot{\mathfrak{F}}_4 - \frac{1}{\eta_4}\tilde{\Theta}_4\dot{\hat{\Theta}}_4 + \vartheta_4^2\sum_{j=1}^{4}h_{4j}^2\left(x_j(t)\right) - \vartheta_4^2\sum_{j=1}^{4}h_{4j}^2\left(x_j\left(t-\sigma_j\right)\right). \tag{72}$$

Integrating (10) and (15) and the fourth equation of (2),

$$\dot{\mathfrak{F}}_4 = \lambda_4\left(c_1x_4 + c_2x_2x_3 + c_3u_d + \chi_4\left(\bar{x}_4\left(t-\sigma_4\right)\right) - \frac{x_4\dot{\nu}_4}{\nu_4}\right). \tag{73}$$

Substituting (73) into (72) leads to

$$\begin{aligned}\dot{V}_4 = \dot{V}_3 &+ \mathfrak{F}_4\lambda_4\left(c_1x_4 + c_2x_2x_3 + c_3u_d + \chi_4\left(\bar{x}_4\left(t-\sigma_4\right)\right) - \frac{x_4\dot{\nu}_4}{\nu_4}\right)\\ &- \frac{1}{\eta_4}\tilde{\Theta}_4\dot{\hat{\Theta}}_4 + \vartheta_4^2\sum_{j=1}^{4}h_{4j}^2\left(x_j(t)\right) - \vartheta_4^2\sum_{j=1}^{4}h_{4j}^2\left(x_j\left(t-\sigma_j\right)\right).\end{aligned} \tag{74}$$

Combining (3) with Young's inequality, we get

$$\mathfrak{F}_4\lambda_4\chi_4\left(\bar{x}_4\left(t-\sigma_4\right)\right) \le \left(\mathfrak{F}_4\lambda_4\right)^2 + \vartheta_4^2\sum_{j=1}^{4}h_{4j}^2\left(x_j\left(t-\sigma_j\right)\right). \tag{75}$$

Inserting (75) into (74) yields

$$\begin{aligned}\dot{V}_4 \le \dot{V}_3 &+ \mathfrak{F}_4\lambda_4\left(c_1x_4 + c_2x_2x_3 + c_3u_d - \frac{x_4\dot{\nu}_4}{\nu_4}\right)\\ &+ \left(\mathfrak{F}_4\lambda_4\right)^2 - \frac{1}{\eta_4}\tilde{\Theta}_4\dot{\hat{\Theta}}_4 + \vartheta_4^2\sum_{j=1}^{4}h_{4j}^2\left(x_j(t)\right).\end{aligned} \tag{76}$$

Introduce function $\Phi_4(Z_4)$ as

$$\Phi_4(Z_4) = c_1 x_4 + c_2 x_2 x_3 + \frac{\mathfrak{J}_2 \lambda_2}{\mathfrak{J}_4 \lambda_4}\left(\left(\frac{a_1}{J} - 1\right)x_3 + \frac{a_2 x_3 x_4}{J}\right) + \frac{b_2 \mathfrak{J}_3 \lambda_3}{\mathfrak{J}_4 \lambda_4} x_2 x_4 + \frac{G_4}{\mathfrak{J}_4 \lambda_4} + \frac{H_4}{\mathfrak{J}_4 \lambda_4}, \tag{77}$$

where $Z_4 = [x_2, x_3, x_4, v_4, \dot{v}_4, \overline{\alpha}_2, \overline{\alpha}_1]^T$, $H_4 = \vartheta_4^2 \sum_{j=1}^{4} h_{4j}^2(x_j(t))$, and $G_4 = \vartheta_4^2 \sum_{j=1}^{4} \int_{t-\tau}^{t} h_{4j}^2(x_j(\sigma))\mathrm{d}\sigma$.

Hence, (76) can be rewritten as

$$\dot{V}_4 \le \dot{V}_3 + \mathfrak{J}_4 \lambda_4 (\Phi_4(Z_4) + c_3 u_d) + \frac{1}{2}(\mathfrak{J}_4 \lambda_4)^2 - \frac{1}{\eta_4}\widetilde{\Theta}_4 \dot{\hat{\Theta}}_4 - G_4, \tag{78}$$

where $\Phi_4(Z_4)$ is a continuous nonlinear function on the compact set $\Omega_{Z_4}$. Based on Lemma 7, $\Phi_4(Z_4)$ can be approximated as

$$\Phi_4(Z_4) = \theta_4^{*T} \psi_4(Z_4) + \delta_4(Z_4), \left|\delta_4(Z_4)\right| \le \overline{\delta}_4. \tag{79}$$

By Young's inequality, we have

$$\mathfrak{J}_4 \lambda_4 \left(\theta_4^{*T} \psi_4(Z_4) + \delta_4(Z_4)\right) \le \frac{1}{2p_4}(\mathfrak{J}_4 \lambda_4)^2 \Theta_4 \psi_4^T(Z_4)\psi_4(Z_4) + \frac{p_4}{2} + \frac{1}{2}(\mathfrak{J}_4 \lambda_4)^2 + \frac{1}{2}\overline{\delta}_4^2, \tag{80}$$

where $p_4$ is a positive constant.

Substituting (79) and (80) into (78) leads to

$$\dot{V}_4 \le \dot{V}_3 + \frac{3}{2}(\mathfrak{J}_4 \lambda_4)^2 + \Theta_4 \psi_4^T(Z_4)\psi_4(Z_4) + \frac{1}{2}\overline{\delta}_4^2 + \mathfrak{J}_4 \lambda_4 c_3 u_d + \frac{1}{2}p_4 - \frac{1}{\eta_4}\widetilde{\Theta}_4 \dot{\hat{\Theta}}_4 - G_4. \tag{81}$$

Construct the adaptive law $\dot{\hat{\Theta}}_4$ and the actual control $u_d$ as

$$\dot{\hat{\Theta}}_4 = \frac{\eta_4}{2p_4}(\mathfrak{J}_4 \lambda_4)^2 \psi_4^T(Z_4)\psi_4(Z_4) - \eta_4 \xi_4 \hat{\Theta}_4, \tag{82}$$

$$u_d = \frac{1}{c_3}\left(-\frac{k_4 \mathfrak{J}_4}{\lambda_4} - \frac{3}{2}\mathfrak{J}_4 \lambda_4 - \frac{1}{2p_4}\mathfrak{J}_4 \lambda_4 \hat{\Theta}_4 \psi_4^T(Z_4)\psi_4(Z_4) + \frac{e_4 \dot{v}_4}{v_4}\right), \tag{83}$$

where $\xi_4, k_4$ are positive constants.

Inserting (82) and (83) into (81) yields

$$\dot{V}_4 \le \dot{V}_3 + \frac{1}{2}p_4 + \frac{1}{2}\overline{\delta}_4^2 - \frac{1}{\eta_4}\widetilde{\Theta}_4 \dot{\hat{\Theta}}_4 - G_4. \tag{84}$$

Similar to (37),

$$\widetilde{\Theta}_4 \hat{\Theta}_4 \le -\frac{1}{2}\widetilde{\Theta}_4^2 + \frac{1}{2}\Theta_4^2. \tag{85}$$

Fusing (70) and (85) into (84) generates

$$\dot{V}_4 \le -\sum_{i=1}^{4} k_i \mathfrak{J}_i^2 - \frac{1}{2}\sum_{i=1}^{4}\widetilde{\Theta}_i^2 - \sum_{i=1}^{4} G_i + \frac{1}{2}\sum_{i=1}^{4}\overline{\delta}_i^2 + \frac{1}{2}\sum_{i=1}^{4} p_i + \frac{1}{2}\sum_{i=1}^{2}\xi_i \Theta_i^2 + \sum_{i=1}^{2}\frac{1}{2}\Upsilon_i^2. \tag{86}$$

*Remark 17.* By constructing suitable Lyapunov–Krasovskii functionals with RBFNNs, the time delays and the unknown nonlinearities in the system are finally eliminated effectively.

## 4. Stability Analysis

For $\forall \Psi > 0$, define the compact sets as

$$\begin{cases} \Omega_1 = \left\{ \left( \mathfrak{F}_1, \tilde{\theta}_1, \mathbb{Z}_1 \right) \colon \mathfrak{F}_1^2 + \dfrac{\tilde{\theta}_1^2}{\eta_1} + 2\mathbb{Z}_1 \le 2\Psi \right\}, \\ \Omega_2 = \left\{ \left( \mathfrak{F}_1, \mathfrak{F}_2, \tilde{\theta}_1, \tilde{\theta}_2, \mathbb{Z}_1, \mathbb{Z}_2 \right) \colon \sum_{i=1}^{2} \mathfrak{F}_i^2 + \sum_{i=1}^{2} \dfrac{\tilde{\theta}_i^2}{\eta_i} + 2\sum_{i=1}^{2} \mathbb{Z}_i \le 2\Psi \right\}, \\ \Omega_3 = \left\{ \left( \mathfrak{F}_i, \tilde{\theta}_i, \mathbb{Z}_i, i = 1, \cdots, 3 \right) \colon \sum_{i=1}^{3} \mathfrak{F}_i^2 + \sum_{i=1}^{3} \dfrac{\tilde{\theta}_i^2}{\eta_i} + 2\sum_{i=1}^{3} \mathbb{Z}_i \le 2\Psi \right\}, \\ \Omega_4 = \left\{ \left( \mathfrak{F}_i, \tilde{\theta}_i, \mathbb{Z}_i, i = 1, \cdots, 4 \right) \colon \sum_{i=1}^{4} \mathfrak{F}_i^2 + \sum_{i=1}^{4} \dfrac{\tilde{\theta}_i^2}{\eta_i} + 2\sum_{i=1}^{4} \mathbb{Z}_i \le 2\Psi \right\}. \end{cases} \tag{87}$$

**Theorem 18.** *In this study, we have constructed the adaptive laws (34), (50), (66), and (82) and the control laws (35), (51), (67), and (83) for the PMSM (2) subject to conditions (11). If the initial conditions fulfill $\Omega_i, i = 1, \ldots, 4$ and $-\underline{\delta} \nu_i(0) < e_i(0) < \overline{\delta} \nu_i(0)$, then all control aims will be achieved.*

*Proof.* Construct the whole Lyapunov function as

$$V = \frac{1}{2}\sum_{i=1}^{4} \mathfrak{F}_i^2 + \sum_{i=1}^{4} \frac{1}{2\eta_i} \tilde{\Theta}_i^2 + \sum_{i=1}^{4}\sum_{j=1}^{4} \int_{t-\sigma_j}^{t} \mathfrak{F}_i^{\,2}(\sigma) h_{ji}^{\,2}\left( \overline{\mathfrak{F}}_i(\sigma) \right) \mathrm{d}\sigma. \tag{88}$$

From (86), we have

$$\begin{aligned} \dot{V} \le & -\sum_{i=1}^{4} k_i \mathfrak{F}_i^{\,2} - \frac{1}{2}\sum_{i=1}^{4} \tilde{\Theta}_i^2 + \frac{1}{2}\sum_{i=1}^{4} \xi_i \Theta_i^{\,2} + \frac{1}{2}\sum_{i=1}^{4} \overline{\delta}_i^{\,2} \\ & + \frac{1}{2}\sum_{i=1}^{2} \Upsilon_i^{\,2} - \sum_{i=1}^{4} \tan h^2\left( \frac{\mathfrak{F}_i}{\hbar_i} \right) G_i + \sum_{i=1}^{4} \left( 1 - 2\tanh^2\left( \frac{\mathfrak{F}_i}{\hbar_i} \right) \right) H_i. \end{aligned} \tag{89}$$

Because $\forall \sigma_j \le \tau, j = 1, \cdots, 4$, it is evident that $[t - \sigma_j, t] \subset [t - \tau, t]$. Thus, we get

$$-G_i \le -\mathbb{Z}_i. \tag{90}$$

Inserting (90) into (89) gets

$$\dot{V} \le -\sum_{i=1}^{4} k_i \mathfrak{F}_i^{\,2} - \frac{1}{2}\sum_{i=1}^{4} \tilde{\Theta}_i^2 + \frac{1}{2}\sum_{i=1}^{4} \xi_i \Theta_i^{\,2} + \sum_{i=1}^{4} \frac{1}{2} \Upsilon_i^{\,2} - \sum_{i=1}^{4} \mathbb{Z}_i + \frac{1}{2}\sum_{i=1}^{4} \overline{\delta}_i^{\,2}. \tag{91}$$

Then, $\dot{V}$ can be described as

$$\dot{V} \le -a_1 V + \Gamma_1, \tag{92}$$

where $\Gamma_1 = (\sum_{i=1}^{4} \overline{\delta}_i^{\,2} + \sum_{i=1}^{4} \xi_i \Theta_i^{\,2} + \sum_{i=1}^{4} \Upsilon_i^{\,2})/2$ and $a_1 = \min\{k_i, \xi_i/2, \Xi/2\}$.

We know that $\lim_{t \longrightarrow \infty} V = \Pi/a_1$, where $\Pi = \max\{\Pi_1, \Pi_2, \Pi_3\}$. Hence, $V$ is ultimately bounded, which assures the boundness of $\Upsilon_1$, $\Upsilon_2$, $\mathfrak{F}_i$, $\tilde{\theta}_i$, and $\sum_{i=1}^{4} \mathfrak{F}_i(\sigma) h_{ji}(\overline{\mathfrak{F}}_i(\sigma))$, $i = 1, \cdots, 4$. According to (14), $\mathfrak{F}_i$ are functions about the variables $e_i$ and $\nu_i$. As $\nu_i$ are bounded-predefined functions, $e_i, i = 1, \cdots, 4$ are bounded. From (16), it is clear that $\hbar_i$ are bounded. The boundedness of $\hat{\Theta}_i$ can be assured based on the boundedness of $\tilde{\Theta}_i$ and $\Theta_i$. According to (35) and (51), we can further conclude that $\alpha_1, \alpha_2, \dot{\alpha}_1, \dot{\alpha}_2$ are bounded, which means that $\overline{\alpha}_1$, $\overline{\alpha}_2$, $\dot{\overline{\alpha}}_1$, and $\dot{\overline{\alpha}}_2$ are also bounded based on (17) and (18). Combining Assumption 4 with (10), the boundness of $x_i, i = 1, \cdots, 4$ can be obtained. Therefore, we can conclude that all signals in the closed-loop PMSM system are uniformly bounded.

Additionally, based on (14), we know that $\mathfrak{I}_i \longrightarrow \pm\infty$ when $e_i \longrightarrow \pm \nu_i$. Because $\mathfrak{I}_i$ are bounded and the initial conditions fulfil $\underline{\delta}\nu_i(0) < e_i(0) < \overline{\delta}\nu_i(0)$, we can get that $-\underline{\delta}\nu_i(t) < e_i(t) < \overline{\delta}\nu_i(t)$ for all $t > 0$. Up to now, the proof of Theorem 1 has been finished. □

## 5. Simulation Examples

In this section, the simulations are presented to prove the validity of the control scheme proposed in this study. The parameters of the PMSM refer to [26] which are listed as $J = 0.003798\text{kg} \cdot m^2, B = 0.001158N \cdot m/(\text{rad}/s), \phi_f = 0.1245\text{Wb}, \quad n_p = 3, L_q = 0.00315H, L_d = 0.00285H, R_s = 0.68\Omega$.

The RBFNNs are introduced to approximate the nonlinear functions during the controller design, in which the Gaussian functions are chosen as $\psi_i(x) = \exp[-(x-\mu_j)(x-\mu_j)/20^2]$, $i = 1, \cdots, 4, j = 1, \cdots, 11$, and the center vector is spaced in the interval $[-20 \quad 20]$. The constants $\overline{\delta}, \underline{\delta}$ are chosen as $\overline{\delta} = \underline{\delta} = 1$. According to the definitions of the control laws $\alpha_1, \alpha_2, u_q, u_d$ and the adaptive laws $\hat{\Theta}_i, i = 1, 2, 3, 4$, respectively, the control design parameters in the simulations are selected as follows by trial and error: $k_1 = 50, k_2 = k_3 = 100, k_3 = 50, p_1 = p_2 = p_4 = 1, p_3 = 0.01, \eta_i = 10, \xi_i = 10, i = 1, \cdots, 4$. The initial values of the PMSM system are $x_1(0) = 0.5, x_2(0) = x_3(0) = x_4(0) = 0$. The reference signal is chosen as $x_d = 0.5\sin(2t) + 0.5\sin(0.5t)$.

*5.1. Example 1.* In order to verify the validity of the proposed time-varying filter, this example considers the full-state prescribed performance control for the PMSM system working under segmented loads, in which the conventional exponential prescribed performance control (EPPC) scheme [9] is chosen to define error bounds as

$$\text{EPPC:} \begin{cases} \nu_{x_1} = 2e^{-2t} + 0.1, \\ \nu_{x_2} = 2e^{-2t} + 1, \\ \nu_{x_3} = 2e^{-2t} + 1.1, \\ \nu_{x_4} = 2e^{-2t} + 0.1. \end{cases} \tag{93}$$

The segmented loads are chosen as

$$\begin{cases} x_{\text{TL}} = 1.2, 0 < t < 10, \\ x_{\text{TL}} = 1.4, 10 \le t < 20, \\ x_{\text{TL}} = 1.2, t \ge 20, \end{cases} \tag{94}$$

and the time-varying filters are selected as

$$\begin{cases} 0.2e^{-0.05t}\dot{\overline{\alpha}}_1 + \overline{\alpha}_1 = \alpha_1, \\ 0.02e^{-0.05t}\dot{\overline{\alpha}}_2 + \overline{\alpha}_2 = \alpha_2. \end{cases} \tag{95}$$

The simulations are compared with the conventional fixed-gain filter in [3, 26], where the filters are set as

$$\begin{cases} 0.2\dot{\overline{\alpha}}_1 + \overline{\alpha}_1 = \alpha_1, \\ 0.02\dot{\overline{\alpha}}_2 + \overline{\alpha}_2 = \alpha_2. \end{cases} \tag{96}$$

The simulation results are shown in Figures 3 and 4. According to Figure 3, it can be found that there are oscillations in the tracking errors, which are generated from the external load perturbations of the PMSM system. The output tracking error $e_1$ has the smallest oscillation (as shown in Figure 3(a)), and the error $e_3$ has the most severe shocks (as shown in Figure 3(c)).

By comparing the performances between the fixed-gain filter and the time-varying filter under the same external abrupt loads, we know that both schemes can obtain good tracking performance with errors constrained in the specified bounds. However, the oscillations of the tracking errors are smaller under the proposed time-varying filters. In Figure 4, it is clear that the time-varying filters can obtain smaller filter errors and ensure superior performance. Given this, we can conclude that the performance of the PMSM system is strongly influenced by external load perturbation. Moreover, our proposed time-varying filter method has better performance than the conventional fixed-gain filter method.

*5.2. Example 2.* This example considers the novel adaptive prescribed performance control (NPPC) for the PMSM system under time-delaying filters (95) with noncontinuous abruptly varying loads (94). To make the prescribed performance function continuous, we choose the first-order filter $F(s) = 1/(1 + 0.05\,\text{s})$ to filter the signal of the external varying loads to obtain the smooth function $\overline{x}_{\text{TL}}$. The simulations are carried out in the following cases:

Case 1: The PMSM works on EPPC, which refers to the literature [9] with the performance functions (93)

Case 2: The PMSM works on CPPC, which refers to the literature [34] with the performance functions

$$\text{CPPC:} \begin{cases} \nu_{x_1} = \text{csch}(t+2) + 0.1, \\ \nu_{x_2} = \text{csch}(t+2) + 1, \\ \nu_{x_3} = \text{csch}(t+2) + 1.1, \\ \nu_{x_4} = \text{csch}(t+2) + 0.1. \end{cases} \tag{97}$$

Case 3: The PMSM works on NPPC, where the performance functions are chosen as

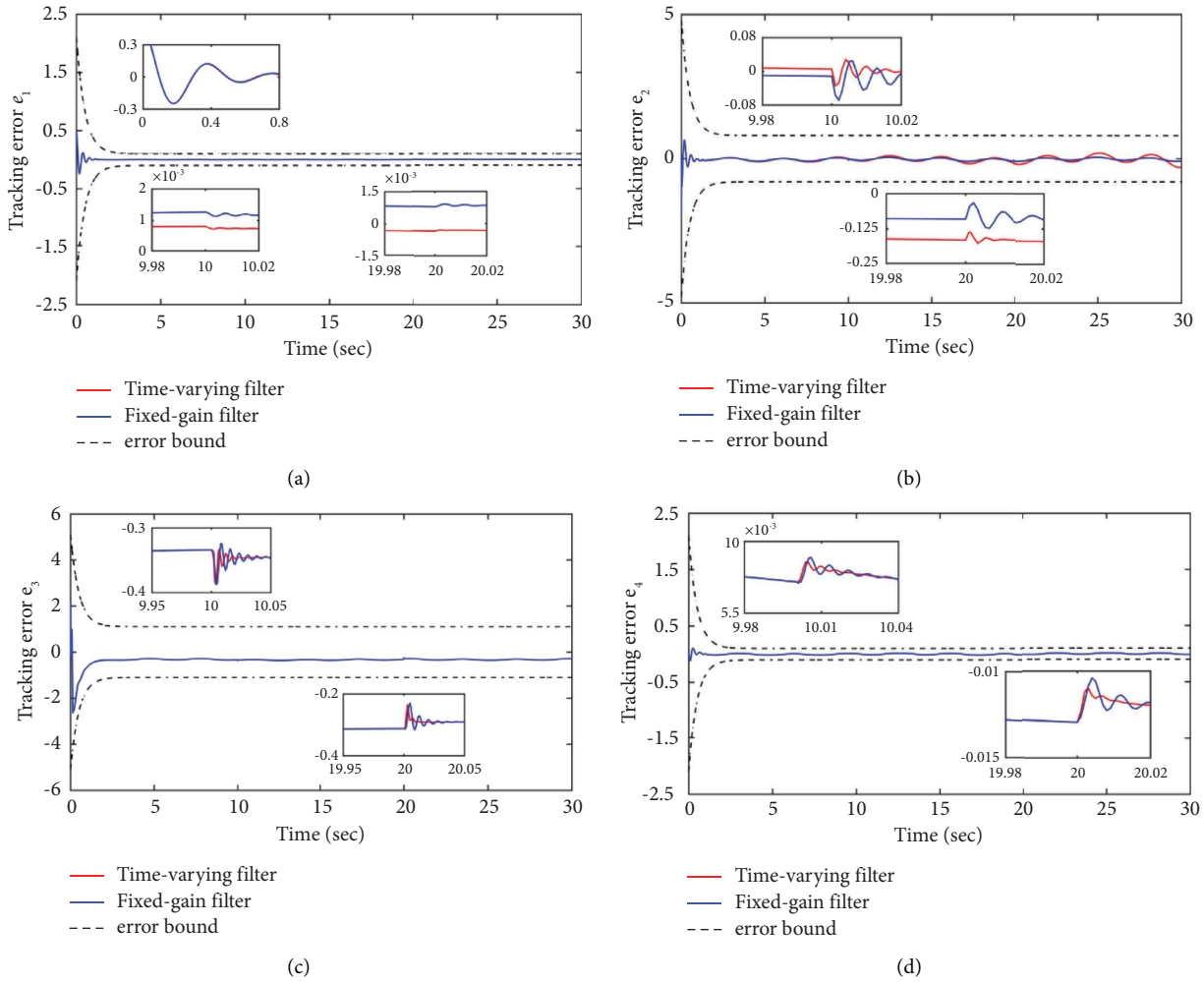


FIGURE 3: The trajectories of tracking errors $e_i, i = 1,2,3,4$ in example 1. (a) The performance of tracking errors $e_1$. (b) The performance of tracking errors $e_2$. (c) The performance of tracking errors $e_3$. (d) The performance of tracking errors $e_4$.

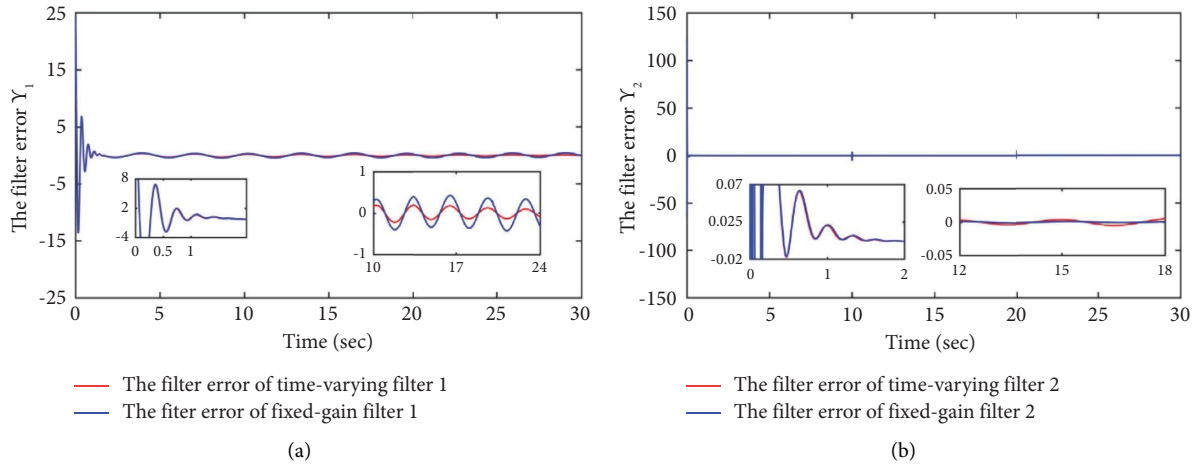


FIGURE 4: The trajectories of filter errors $\Upsilon_i, i = 1,2$ in example 1. (a) The trajectories of filter error $\Upsilon_1$. (b) The trajectories of filter error $\Upsilon_2$.

$$\text{NPPC: } \begin{cases} \nu_{x_1} = 2(t+e)^{-2t} + 0.1 + 0.15\tan h\left(\dot{\bar{x}}_{\text{TL}}{}^2\right), \\ \nu_{x_2} = 2(t+e)^{-2t} + 1 + 0.15\tan h\left(\dot{\bar{x}}_{\text{TL}}{}^2\right), \\ \nu_{x_3} = 2(t+e)^{-2t} + 1.1 + 0.15\tan h\left(\dot{\bar{x}}_{\text{TL}}{}^2\right), \\ \nu_{x_4} = 2(t+e)^{-2t} + 0.1 + 0.15\tan h\left(\dot{\bar{x}}_{\text{TL}}{}^2\right). \end{cases} \tag{98}$$

Case 4: The PMSM works on NPPC with time delays as

$$\text{Time delays: } \begin{cases} \chi_1(x(t-\sigma_1)) = 0.1x_1^2(t-0.5), \\ \chi_2(\bar{x}_2(t-\sigma_2)) = 0.3x_1{}^2(t-0.6)x_2(t-0.6), \\ \chi_3(\bar{x}_3(t-\sigma_3)) = 0.2x_2(t-0.7)x_1{}^2(t-0.7)x_3{}^2(t-0.7), \\ \chi_4(\bar{x}_4(t-\sigma_4)) = 5x_4{}^3(t-0.8)x_1(t-0.8)^2x_2(t-0.8)x_3(t-0.8). \end{cases} \tag{99}$$

Functions $h_{\text{ij}}$ can be set as

$$\begin{cases} h_{11} = x_1{}^2, \\ h_{21} + h_{22} = x_1{}^2|x_2|, \\ h_{31} + h_{32} + h_{33} = x_1{}^2x_3{}^2|x_2|, \\ h_{41} + h_{42} + h_{43} + h_{44} = 10|x_4|^3x_1{}^2|x_2||x_3|. \end{cases} \tag{100}$$

*Remark 19.* The EPPC, CPPC, and NPPC have the same initial and final values of the performance function for each state, and the same log-type transformation (14) is adopted to convert constrained problems to unconstrained problems. Based on this, the fairness of the comparison experiment is guaranteed.

*Remark 20.* The performance of tracking errors $e_i, i = 1, \cdots, 4$ is visual measures of controlling abilities. From (14), it can be concluded that $e_i = (1 - 2/(1 + e^{2\mathfrak{F}_i}))\nu_i$. Combining $\lim_{t \longrightarrow \infty} V = \Pi/a_1$ with (88), we can get $|\mathfrak{F}_i| \leq \sqrt{2\Pi/a_1}$. It is evident that $1 - 2/(1 + e^{2\mathfrak{F}_i})$ are monotonically increasing functions of variables $\mathfrak{F}_i$. Then, we can further get $(1 - 2/(1 + e^{-2\sqrt{2\Pi/a_1}}))\nu_i \leq e_i \leq (1 - 2/(1 + e^{2\sqrt{2\Pi/a_1}}))\nu_i$. According to (12), the values of $\nu_i$ are small enough by increasing parameters $\kappa_i, \rho$ and reducing parameters $\nu_{i\infty}, \ell_2, \ell_3$. As a result, the tracking errors $e_i$ can be tuned arbitrarily small to obtain a better performance theoretically. However, it will also increase the burden of the controller or even cause unresolvable situations. Therefore, a balance between system performance and control effort should be maintained.

The simulation results are shown in Figures 5–9. From Figure 5, we can see that the output $x_1$ of EPPC, CPPC, NPPC, and NPPC with time delays can track the reference signal $x_d$ effectively.

Figure 6 reveals the full-state prescribed performance of the PMSM system. By analyzing EPPC, CPPC, and NPPC, it is clear that the performance boundaries of NPPC can be adaptively adjusted to offset the oscillations generated by external load changes, and the fastest convergence errors can be obtained. In contrast, Figure 6(c) shows that the tracking error trajectory of CPPC has already exceeded the error bounds of NPPC in the transient state. By comparing the tracking performance of NPPC and NPPC with time delays, it is evident that the proposed controller can achieve the control objective even when time delay disturbances are present.

The trajectories of the control laws are given in Figure 7, and it can be found that although the disturbance of the external loads leads to the chattering of the control laws, where the NPPC with time delays has the largest vibrations, all control laws of the system are being within the reasonable range. As can be seen in Figure 8, $\Theta_i, i = 1,2,3,4$ are bounded, which means that the weights of RBFNNs in this study are bounded. From Figure 9, we know that the filtering error of the system can converge to zero within a certain time by the proposed time-varying filters.

*5.3. Example 3.* This example considers the novel adaptive prescribed performance control (NPPC) for the PMSM system under time-delay filters (95) with continuously varying loads and time delays, where the loads are

$$x_{\text{TL}} = 1.5\sin(2t). \tag{101}$$

Similarly, comparative experiments are conducted for the following four scenarios: EPPC with performance functions (93), CPPC with performance functions (97), NPPC with performance functions (98), and NPPC with time delays (99).

The simulation results are presented in Figures 10–14. From Figure 10, it can be seen that NPPC, EPPC, and CPPC can track the reference signal effectively. From Figure 11, it is clear that the tracking errors of NPPC can converge in a shorter time and obtain better performance than EPPC and CPPC, where Figure 11(c) shows that the trajectory of the tracking error in the CPPC almost exceeds the error bounds of the NPPC during the transient state. What's more, the performance bounds of the NPPC can adaptively adjust to counteract the oscillations generated by the external load.

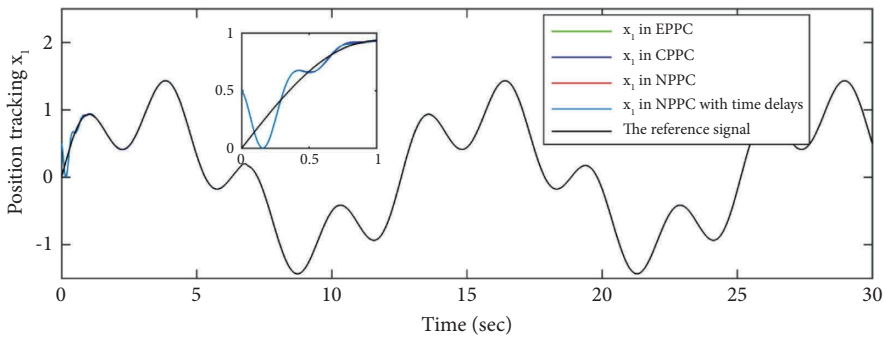


FIGURE 5: The $x_1$ tracking performance in example 2.

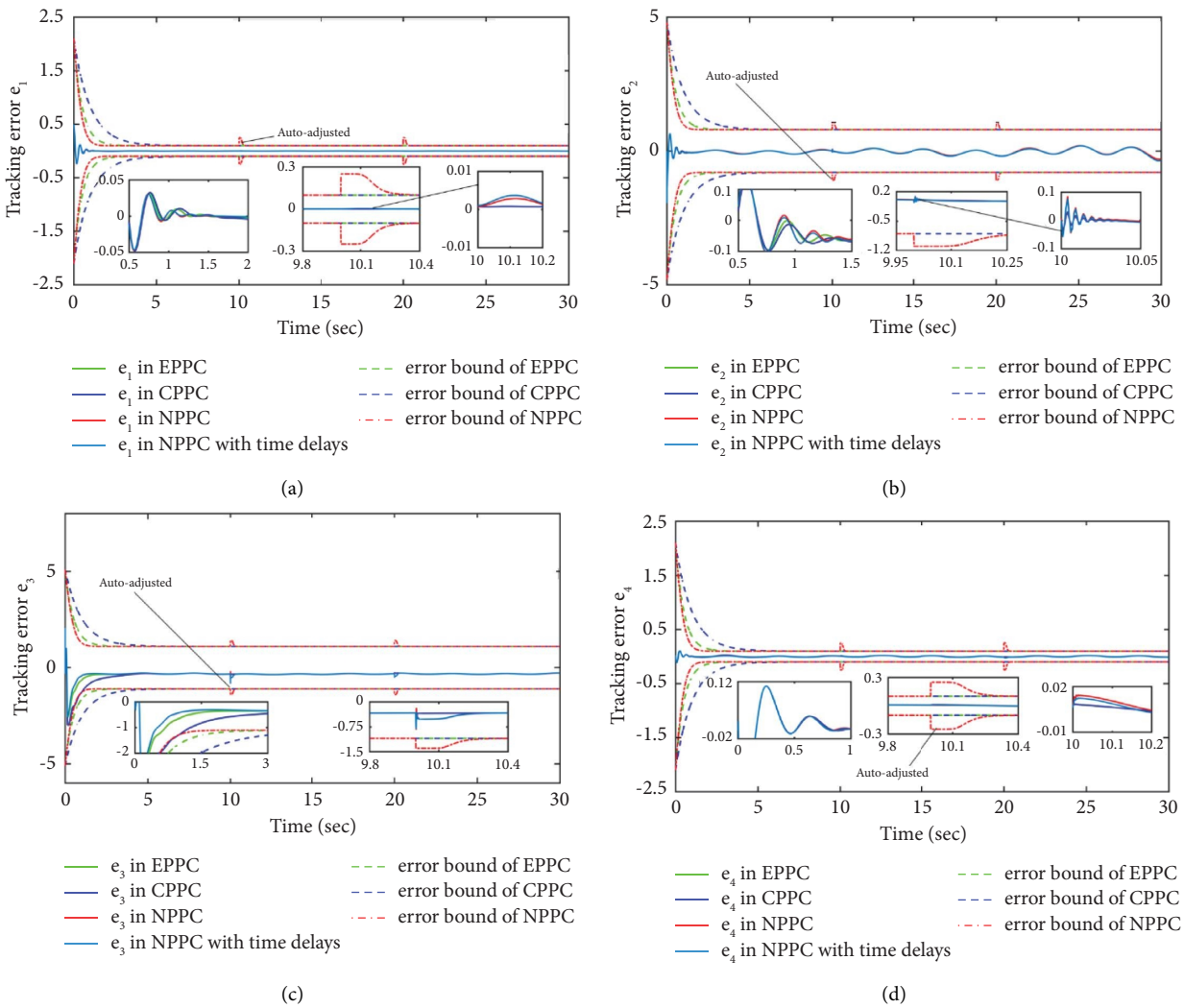


FIGURE 6: The trajectories of tracking errors $e_i, i = 1,2,3,4$ in example 2. (a) The performance of tracking errors $e_1$. (b) The performance of tracking errors $e_2$. (c) The performance of tracking errors $e_3$. (d) The performance of tracking errors $e_4$.

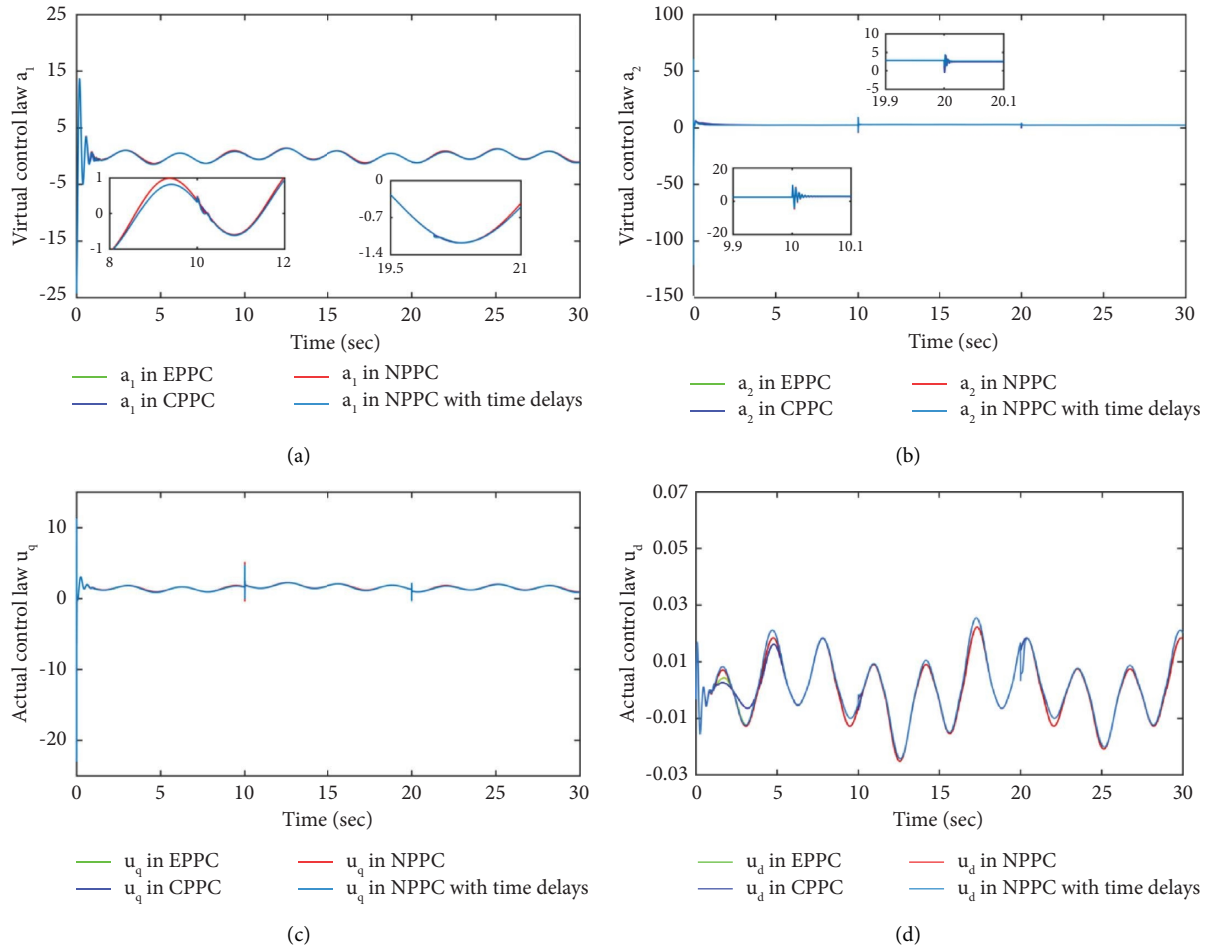


Figure 7: The trajectories of control laws in example 2. (a) The trajectories of control laws $\alpha_1$. (b) The trajectories of control laws $\alpha_2$. (c) The trajectories of control laws $u_q$. (d) The trajectories of control laws $u_d$.

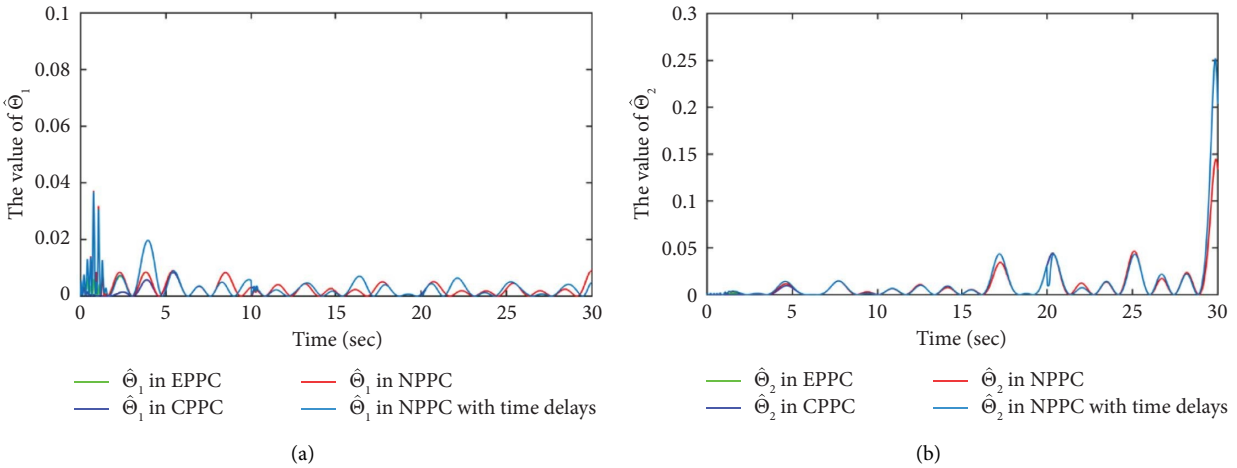


Figure 8: Continued.

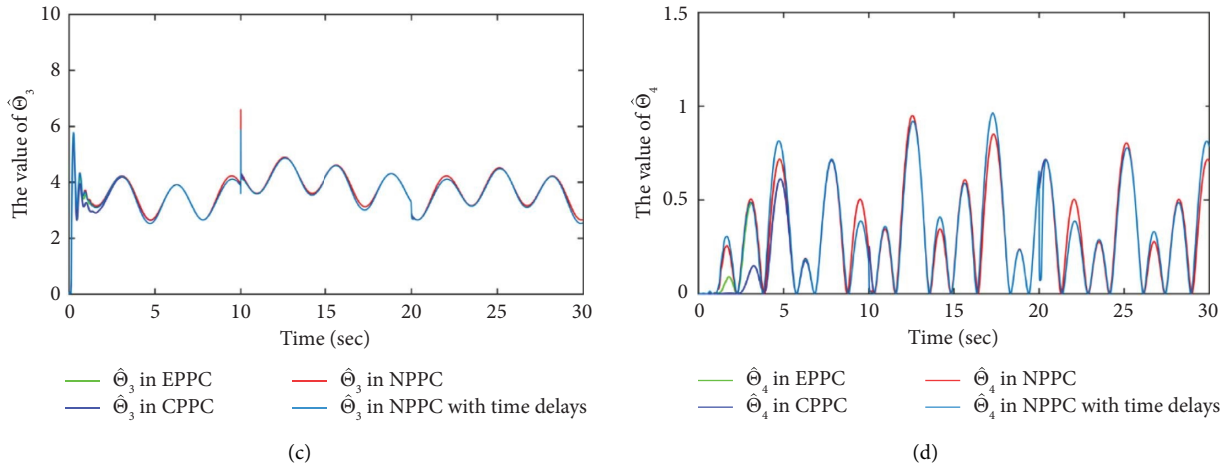


FIGURE 8: The trajectories of $\hat{\Theta}_i, i = 1,2,3,4$ in example 2. (a) The trajectories of $\hat{\Theta}_1$. (b) The trajectories of $\hat{\Theta}_2$. (c) The trajectories of $\hat{\Theta}_3$. (d) The trajectories of $\hat{\Theta}_4$.

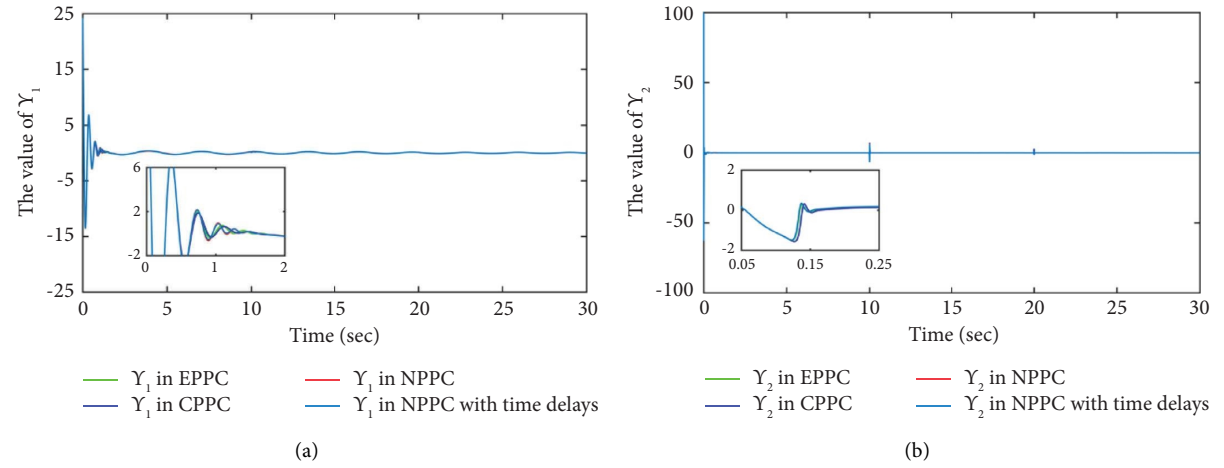


FIGURE 9: The trajectories of filter errors $\Upsilon_i, i = 1,2$ in example 2. (a) The trajectories of filter errors $\Upsilon_1$. (b) The trajectories of filter errors $\Upsilon_2$.

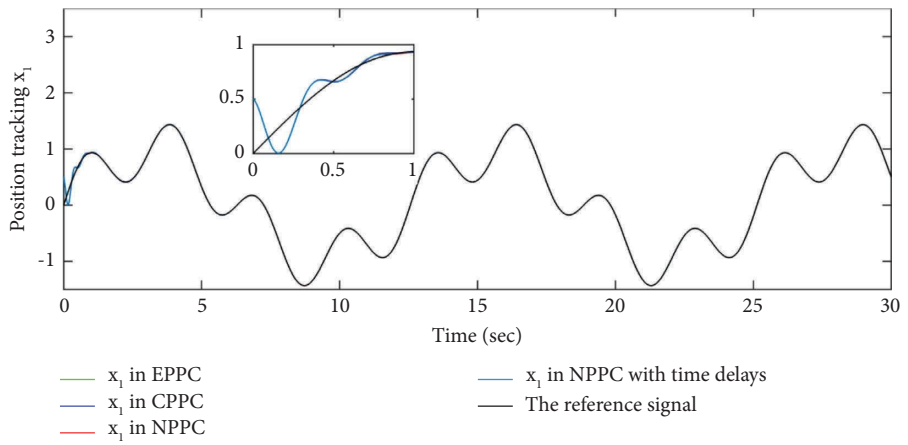


FIGURE 10: The $x_1$ tracking performance in example 3.

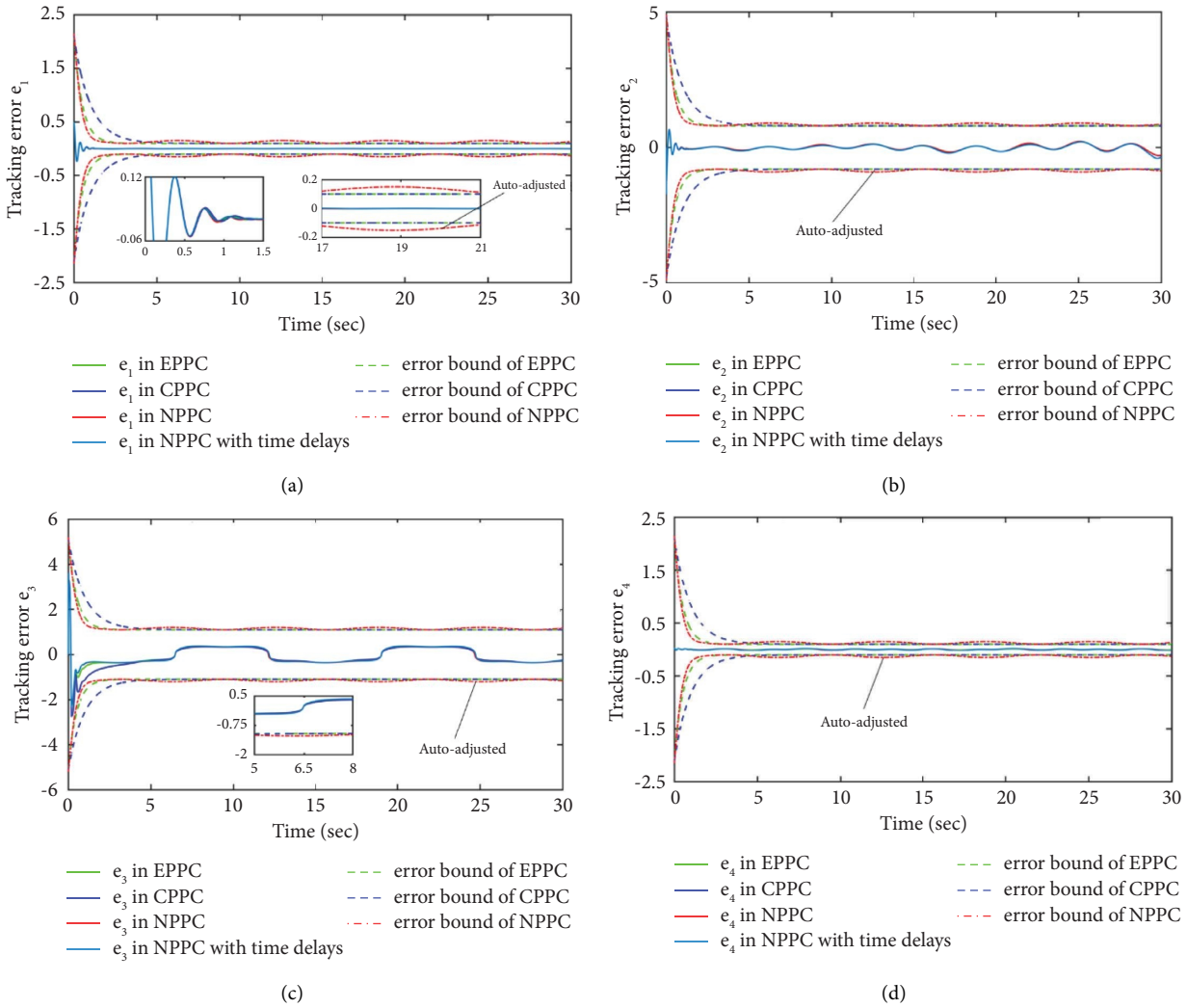


Figure 11: The trajectories of tracking errors $e_i, i = 1,2,3,4$ in example 3. (a) The performance of tracking errors $e_1$. (b) The performance of tracking errors $e_2$. (c) The performance of tracking errors $e_3$. (d) The performance of tracking errors $e_4$.

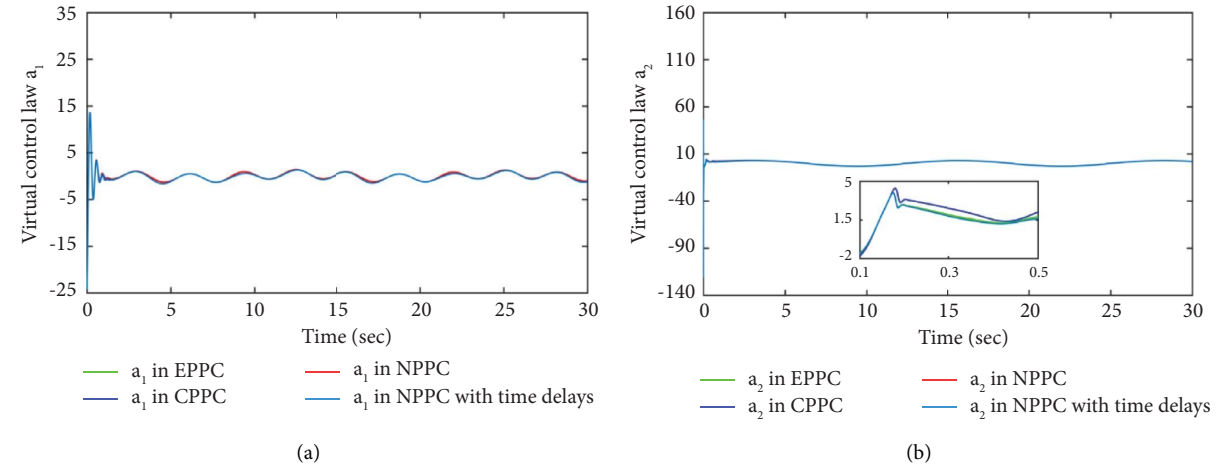


Figure 12: Continued.

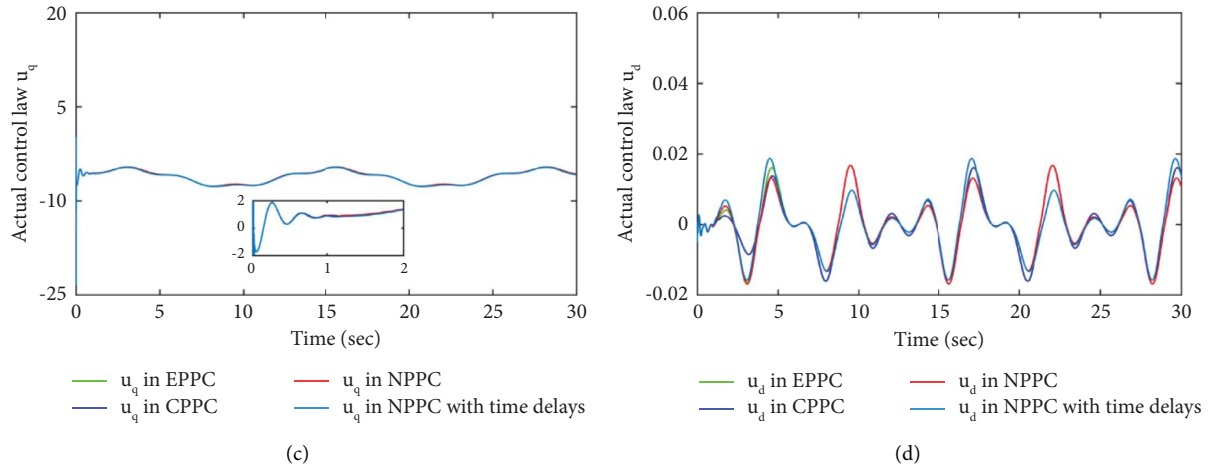


FIGURE 12: The trajectories of control laws in example 3. (a) The trajectories of control laws $\alpha_1$. (b) The trajectories of control laws $\alpha_2$. (c) The trajectories of control laws $u_q$. (d) The trajectories of control laws $u_d$.

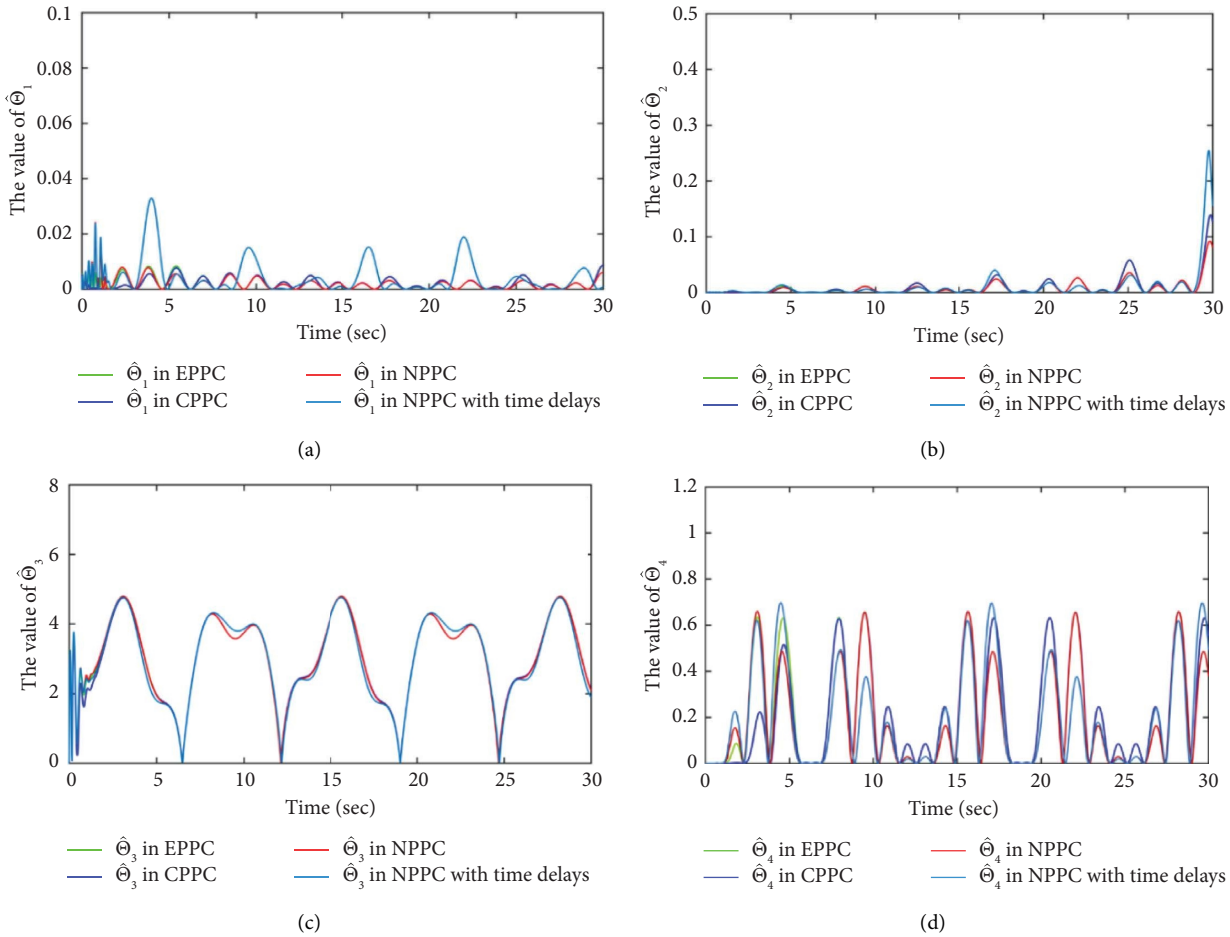


FIGURE 13: The trajectories of $\hat{\Theta}_i, i = 1,2,3,4$ in example 3. (a) The trajectories of $\hat{\Theta}_1$. (b) The trajectories of $\hat{\Theta}_2$. (c) The trajectories of $\hat{\Theta}_3$. (d) The trajectories of $\hat{\Theta}_4$.

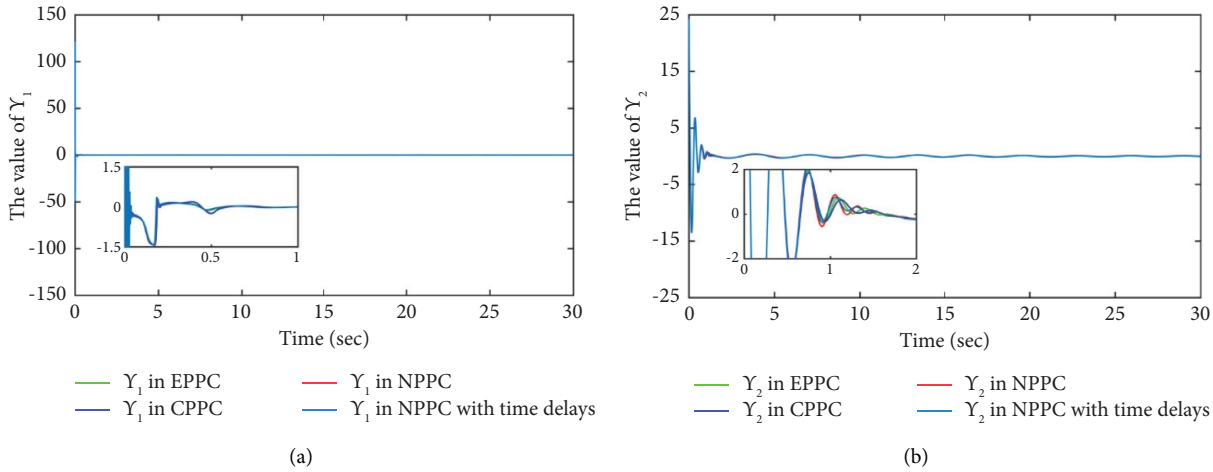


FIGURE 14: The trajectories of filter error $\Upsilon_i, i = 1,2$ in example 3. (a) The trajectories of filter errors $\Upsilon_1$. (b) The trajectories of filter errors $\Upsilon_2$.

Figure 12 shows that all control laws in NPPC, NPPC with time delays, EPPC, and CPPC under the condition of continuously varying loads are within the reasonable range. Among them, the NPPC has a milder shock. As can be seen in Figure 13, $\Theta_i, i = 1,2,3,4$ are bounded. From Figure 14, it is clear that the filtering errors of the system can converge to zero in a certain time by the proposed time-varying filtering.

According to the abovementioned three simulation examples, we know that the external load perturbations have a significant impact on system performance, and the control system with time-varying filters can obtain better performance than the traditional first-order filtering method. In addition, the control scheme proposed in this study can effectively solve the time-delay problem of the system under the disturbance of segmented load and continuously changing load.

## 6. Conclusions

In this study, a neuro-learning-based adaptive prescribed performance control scheme is proposed to solve the tracking problem for the PMSM with full-state constraints, external load disturbances, and time delays. First, with the improved PPC for the PMSM, the tracking errors are well bounded in the preset boundaries, and the controller can tune automatically to circumvent the overrun and high frequently chattering of external loads. Second, via constructing proper Lyapunov–Krasovskii functionals with RBFNNs, time-delay terms and the nonlinearities in the system have been handled effectively. Meanwhile, the time-varying filters are introduced into the backstepping control to bypass the "complexity explosion." Then, the stability analysis demonstrates that all signals in the closed-loop system are bounded, and the tracking errors are within the prescribed boundaries. At last, the simulation results illustrate the effectiveness of the suggested scheme.

Future work will focus on extending such design into broad applications to realize finite-time or fixed-time prescribed performance control for systems with full-state constraints and time delays which are commonly experienced in real scenarios.

## Data Availability

The data supporting the current study are available from the corresponding author upon request.

## Conflicts of Interest

The authors declare that they have no conflicts of interest.

## Acknowledgments

This work was supported in part by the Key Technologies Research and Development Program (2020YFB1713300, 52275480, and 2018AAA0101803) and Guizhou Provincial Department of Science and Technology Project Funding ([2023]02).

## References

[1] X. Li, W. Tian, X. Gao, Q. Yang, and R. Kennel, "A generalized observer-based robust predictive current control strategy for PMSM drive system," *IEEE Transactions on Industrial Electronics*, vol. 69, no. 2, pp. 1322–1332, 2022.

[2] Q. Chen, X. Yu, M. Sun, C. Wu, and Z. Fu, "Adaptive repetitive learning control of PMSM servo systems with bounded nonparametric uncertainties: theory and experiments," *IEEE Transactions on Industrial Electronics*, vol. 68, no. 9, pp. 8626–8635, 2021.

[3] Z. Lv, Y. Ma, J. Liu, and J. Yu, "Full-state constrained adaptive fuzzy finite-time dynamic surface control for PMSM drive systems," *International Journal of Fuzzy Systems*, vol. 23, no. 3, pp. 804–815, 2021.

[4] S. Wu, J. Zhang, and B. Chai, "A robust backstepping sensorless control for interior permanent magnet synchronous motor using a super-twisting based torque observer," *Asian Journal of Control*, vol. 21, no. 1, pp. 172–183, 2019.

[5] X. Liu and H. Yu, "Continuous adaptive integral-type sliding mode control based on disturbance observer for PMSM drives," *Nonlinear Dynamics*, vol. 104, no. 2, pp. 1429–1441, 2021.

[6] Y. Deng, J. Wang, H. Li, J. Liu, and D. Tian, "Adaptive sliding mode current control with sliding mode disturbance observer

for PMSM drives," *ISA Transactions*, vol. 88, pp. 113–126, 2019.

[7] J. Song, W. X. Zheng, and Y. Niu, "Self-triggered sliding mode control for networked PMSM speed regulation system: a PSO-optimized super-twisting algorithm," *IEEE Transactions on Industrial Electronics*, vol. 69, no. 1, pp. 763–773, 2022.

[8] B. Xu, L. Zhang, and W. Ji, "Improved non-singular fast terminal sliding mode control with disturbance observer for PMSM drives," *IEEE Transactions on Transportation Electrification*, vol. 7, no. 4, pp. 2753–2762, 2021.

[9] Y. Dai, S. Ni, D. Xu, L. Zhang, and X.-G. Yan, "Disturbance-observer based prescribed-performance fuzzy sliding mode control for PMSM in electric vehicles," *Engineering Applications of Artificial Intelligence*, vol. 104, Article ID 104361, 2021.

[10] Y. Yao, Y. Huang, F. Peng, and J. Dong, "A sliding-mode position estimation method with chattering suppression for LCL-equipped high-speed surface-mounted PMSM drives," *IEEE Transactions on Power Electronics*, vol. 37, pp. 2057–2071, 2021.

[11] W. Chang and S. Tong, "Adaptive fuzzy tracking control design for permanent magnet synchronous motors with output constraint," *Nonlinear Dynamics*, vol. 87, no. 1, pp. 291–302, 2017.

[12] X. Wang and S. Wang, "Adaptive fuzzy robust control of PMSM with smooth inverse based dead-zone compensation," *International Journal of Control, Automation and Systems*, vol. 14, no. 2, pp. 378–388, 2016.

[13] M. Zou, J. Yu, Y. Ma, L. Zhao, and C. Lin, "Command filtering-based adaptive fuzzy control for permanent magnet synchronous motors with full-state constraints," *Information Sciences*, vol. 518, pp. 1–12, 2020.

[14] J. Z. Yang, Y. X. Li, and S. Tong, "Adaptive NN finite-time tracking control for PMSM with full state constraints," *Neurocomputing*, vol. 443, pp. 213–221, 2021.

[15] S. Cheng, J. Yu, C. Lin, L. Zhao, and Y. Ma, "Neuroadaptive finite-time output feedback control for PMSM stochastic nonlinear systems with iron losses via dynamic surface technique," *Neurocomputing*, vol. 402, pp. 162–170, 2020.

[16] G. Feng, C. Lai, and N. C. Kar, "Speed harmonic based modeling and estimation of permanent magnet temperature for PMSM drive using kalman filter," *IEEE Transactions on Industrial Informatics*, vol. 15, no. 3, pp. 1372–1382, 2019.

[17] J. Wu and R. Ma, "Robust finite-time and fixed-time chaos synchronization of PMSMs in noise environment," *ISA Transactions*, vol. 119, pp. 65–73, 2022.

[18] B. Selma, S. Chouraqui, and H. Abouaïssa, "Fuzzy swarm trajectory tracking control of unmanned aerial vehicle," *Journal of Computational Design and Engineering*, vol. 7, no. 4, pp. 435–447, 2020.

[19] X. Zhang, R. Shi, Z. Zhu, and Y. Quan, "Adaptive nonsingular fixed-time sliding mode control for manipulator systems' trajectory tracking," *Complex Intell. Syst.*, vol. 9, no. 2, pp. 1605–1616, 2022.

[20] E. Muñoz-Palomeque, J. E. Sierra-García, and M. Santos, "Wind turbine maximum power point tracking control based on unsupervised neural networks," *Journal of Computational Design and Engineering*, vol. 10, no. 1, pp. 108–121, 2023.

[21] S. Gao, H. Dong, B. Ning, T. Tang, and Y. Li, "Nonlinear mapping-based feedback technique of dynamic surface control for the chaotic PMSM using neural approximation and parameter identification," *IET Control Theory & Applications*, vol. 12, no. 6, pp. 819–827, 2018.

[22] M. Chen, H. Wang, and X. Liu, "Adaptive fuzzy practical fixed-time tracking control of nonlinear systems," *IEEE Transactions on Fuzzy Systems*, vol. 29, no. 3, pp. 664–673, 2021.

[23] Q. Jiang, J. Liu, J. Yu, and C. Lin, "Full state constraints and command filtering-based adaptive fuzzy control for permanent magnet synchronous motor stochastic systems," *Information Sciences*, vol. 567, pp. 298–311, 2021.

[24] F. Zhang, W. Wu, and C. Wang, "Pattern-based learning and control of nonlinear pure-feedback systems with prescribed performance," *Science China Information Sciences*, vol. 66, no. 1, Article ID 112202, 2023.

[25] J. Yu, P. Shi, W. Dong, B. Chen, C. Lin, and C. Lin, "Neural network-based adaptive dynamic surface control for permanent magnet synchronous motors," *IEEE Transactions on Neural Networks and Learning Systems*, vol. 26, no. 3, pp. 640–645, 2015.

[26] Y. Yu, L. Ding, and W. Wang, "Finite-time composite adaptive fuzzy control of permanent magnet synchronous motors," *International Journal of Fuzzy Systems*, vol. 24, no. 1, pp. 135–146, 2022.

[27] L. Ding, W. Wang, and Y. Yu, "Finite-time adaptive NN control for permanent magnet synchronous motors with full-state constraints," *Neurocomputing*, vol. 449, pp. 435–442, 2021.

[28] M. M. Zirkohi, "Command filtering-based adaptive control for chaotic permanent magnet synchronous motors considering practical considerations," *ISA Transactions*, vol. 114, pp. 120–135, 2021.

[29] Q. Chen, Y. Ye, Z. Hu, J. Na, and S. Wang, "Finite-time approximation-free attitude control of quadrotors: theory and experiments," *IEEE Transactions on Aerospace and Electronic Systems*, vol. 57, no. 3, pp. 1780–1792, 2021.

[30] Y. Wang, J. Hu, J. Wang, and X. Xing, "Adaptive neural novel prescribed performance control for non-affine pure-feedback systems with input saturation," *Nonlinear Dynamics*, vol. 93, no. 3, pp. 1241–1259, 2018.

[31] C. X. Wang, Y. Q. Wu, Y. Zhao, and J. L. Yu, "Asymptotic tracking control for time-delay nonlinear systems with parametric uncertainties and full state constraints," *ISA Transactions*, vol. 98, pp. 101–109, 2020.

[32] C. Hua, G. Liu, Y. Li, and X. Guan, "Adaptive neural tracking control for interconnected switched systems with non-ISS unmodeled dynamics," *IEEE Transactions on Cybernetics*, vol. 49, no. 5, pp. 1669–1679, 2019.

[33] F. Jia, C. Lei, J. Lu, and Y. Chu, "Adaptive prescribed performance output regulation of nonlinear systems with nonlinear exosystems," *International Journal of Control, Automation and Systems*, vol. 18, no. 8, pp. 1946–1955, 2020.

[34] Y. Wang and J. Hu, "Improved prescribed performance control for air-breathing hypersonic vehicles with unknown deadzone input nonlinearity," *ISA Transactions*, vol. 79, pp. 95–107, 2018.

[35] X. Wang, B. Niu, X. Song, P. Zhao, and Z. Wang, "Neural networks-based adaptive practical preassigned finite-time fault tolerant control for nonlinear time-varying delay systems with full state constraints," *International Journal of Robust and Nonlinear Control*, vol. 31, no. 5, pp. 1497–1513, 2021.

[36] B. Niu, H. Li, T. Qin, and H. R. Karimi, "Adaptive NN dynamic surface controller design for nonlinear pure-feedback switched systems with time-delays and quantized input," *IEEE Trans. Syst. Man, Cybern. Syst.*, vol. 48, no. 10, pp. 1676–1688, 2018.

[37] Y. H. Choi and S. J. Yoo, "Minimal-approximation-based decentralized backstepping control of interconnected time-delay systems," *IEEE Transactions on Cybernetics*, vol. 46, no. 12, pp. 3401–3413, 2016.

[38] S. Li, C. K. Ahn, and Z. Xiang, "Adaptive fuzzy control of switched nonlinear time-varying delay systems with prescribed performance and unmodeled dynamics," *Fuzzy Sets and Systems*, vol. 371, pp. 40–60, 2019.

[39] H. Gao, T. Zhang, and X. Xia, "Adaptive neural control of stochastic nonlinear systems with unmodeled dynamics and time-varying state delays," *Journal of the Franklin Institute*, vol. 351, no. 6, pp. 3182–3199, 2014.

[40] T. Zhang, M. Xia, and Y. Yi, "Adaptive neural dynamic surface control of strict-feedback nonlinear systems with full state constraints and unmodeled dynamics," *Automatica*, vol. 81, pp. 232–239, 2017.

[41] M. Van and S. S. Ge, "Adaptive fuzzy integral sliding-mode control for robust fault-tolerant control of robot manipulators with disturbance observer," *IEEE Transactions on Fuzzy Systems*, vol. 29, no. 5, pp. 1284–1296, 2021.

[42] Q. Zhou, S. Zhao, H. Li, R. Lu, and C. Wu, "Adaptive neural network tracking control for robotic manipulators with dead zone," *IEEE Transactions on Neural Networks and Learning Systems*, vol. 30, no. 12, pp. 3611–3620, 2019.

[43] J. Zhang, B. Niu, D. Wang, H. Wang, P. Zhao, and G. Zong, "Time-/event-triggered adaptive neural asymptotic tracking control for nonlinear systems with full-state constraints and application to a single-link robot," *IEEE Transactions on Neural Networks and Learning Systems*, vol. 33, no. 11, pp. 6690–6700, 2022.

[44] R. Jon, Z. Wang, C. Luo, and M. Jong, "Adaptive robust speed control based on recurrent elman neural network for sensorless PMSM servo drives," *Neurocomputing*, vol. 227, pp. 131–141, 2017.